Chemical Engineering Journal 506 (2025) 160030

Contents lists available at ScienceDirect

Chemical Engineering Journal

journal homepage: www.elsevier.com/locate/cej

Mechanistic insights into D-cyphenothrin biodegradation by *Rhodococcus ruber* Y14 and its potential for bioremediation of pyrethroid-polluted environment

Yaohua Huang [a,b,1], Shunkang Zhou [a,b,1], Wen-Juan Chen [a,b,1], Xiaofan Zhou [a,b], Shao-Fang Chen [a,b], Haoran Song [a,b], Zhenchen Yan [a,b], Sandhya Mishra [c], Mohamed A. Ghorab [d,e], Pankaj Bhatt [a,b], Shaohua Chen [a,b,*]

[a] State Key Laboratory of Green Pesticide, Guangdong Province Key Laboratory of Microbial Signals and Disease Control, Integrative Microbiology Research Centre, South China Agricultural University, Guangzhou 510642 China
[b] College of Plant Protection, South China Agricultural University, Guangzhou 510642 China
[c] Environmental Technologies Division, CSIR-National Botanical Research Institute (NBRI), Rana Pratap Marg, Lucknow 226001 India
[d] Wildlife Toxicology Lab, Department of Animal Science, Institute for Integrative Toxicology (IIT), Michigan State University, East Lansing, MI 48824, USA
[e] Department of Molecular Biosciences, School of Veterinary Medicine, University of California Davis, Davis, CA 95616-8741, USA

ARTICLE INFO

Keywords:
Biodegradation
Pyrethroids
D-cyphenothrin
Carboxylesterase
Rhodococcus

ABSTRACT

Persistent use of pyrethroid insecticides has resulted in heavy environmental contamination worldwide. However, the currently available pyrethroid degrading microbes are not optimal. In addition, the degradation mechanisms and metabolic behaviors of the pyrethroid D-cyphenothrin are poorly understood. In this study, a novel Actinomycete strain, *Rhodococcus ruber* Y14, was shown to completely degrade multiple pyrethroid insecticides including D-cyphenothrin, allethrin, fenvalerate, tetramethrin, and prallethrin within a short period. Four metabolites, including chrysanthemic acid, 2-(3-hydroxyphenyl)acetonitrile, 3-phenoxybenzaldehyde, and phenylmethanol from the degradation of D-cyphenothrin were identified, suggesting that carboxyl bond hydrolysis is the main degradation pathway involved. Toxicological assessments indicated that the hydrolysis transformation process of D-cyphenothrin was a detoxification process. Y14 demonstrated efficient soil bioremediation by removing over 80 % of D-cyphenothrin (50 mg/kg) from both sterile and non-sterile soils within 25 days, with significantly reduced half-lives. High-throughput soil sequencing revealed that indigenous microorganisms, predominant *Sphingomonas* and *Sinomonas*, synergistically declined the half-life of D-cyphenothrin in soil (<6.9 d) with Y14. Through proteomics and genome annotation, a degradation gene *dcyR* was identified from Y14, which encodes a 55.92 kDa carboxylesterase that exhibits significant catalytic activity toward D-cyphenothrin. Molecular docking and site-directed mutagenesis revealed that DcyR contains a conserved pentapeptide motif (G-E-S-S-G), with Ser193 as the catalytic site for the catalytic triad (Asp315-Ser193-His417). Through the nucleophilic attack of the serine hydroxyl, D-cyphenothrin was decomposed into α-hydroxy-3-phenoxy-benzeneacetonitrile and chrysanthemic acid, which were further degraded into non-toxic small molecule substances. These findings will significantly enhance our understanding of the microbial catabolism of the widely used pyrethroid D-cyphenothrin at the molecular level and provide potential candidates for the development of effective pyrethroid bioremediation strategies.

1. Introduction

A pyrethroid insecticide is a synthetic analog of natural pyrethrins, the first-generation product of which was allethrin, synthesized in 1949 [1]. Subsequently, it was found that first-generation synthetic pyrethroids were photolabile, easily photodegrading in the natural

* Corresponding author at: State Key Laboratory of Green Pesticide, Integrative Microbiology Research Centre, South China Agricultural University, Guangzhou 510642, China.
E-mail address: shchen@scau.edu.cn (S. Chen).
[1] These authors contributed equally to this work.

https://doi.org/10.1016/j.cej.2025.160030
Received 30 September 2024; Received in revised form 22 January 2025; Accepted 27 January 2025
Available online 30 January 2025

environment [2]. Therefore, in the 1970 s, a cyano group was introduced into the pyrethroid structure at the α-chiral carbon site, resulting in the second generation of pyrethroid insecticides, such as D-cyphenothrin [3]. Pyrethroid insecticides have been used worldwide for half a century; however, the World Health Organization (WHO) phased out carbamate and organophosphorus insecticides with high toxicity and high residue, so the global market share of pyrethroid insecticides has reached a new high in recent years [4], accounting for about 30 % of the global insecticide market according to 2018 statistics [5].

Pyrethroid insecticides represent a category of non-polar pesticides [6]. After application, less than 1 % of the active ingredients in pyrethroids reach the target organisms, with most entering the natural environment due to various factors [7]. When pyrethroid insecticides enter the soil surface, parts of them decompose through natural photolysis, and most of them are adsorbed into the soil structure [8]. The unnecessarily long-term use of pyrethroid insecticides has led to widespread reports of pyrethroid residues worldwide [9]. High concentrations of bifenthrin and *trans*-permethrin have been detected at rates of 74 and 100 %, respectively, in the surface water and sediment of multiple watersheds in southern California [10,11].

Increasing amounts of pyrethroid residues enter natural water bodies through surface runoff and groundwater migration [11]. With the biomagnification of aquatic food webs, as well as measures such as agricultural irrigation, pyrethroid pesticide residues will eventually accumulate in the human body [12]. Studies by Djouaka et al. [13] showed that cyhalothrin residue, detected in lettuce and cabbage purchased from local vegetable markets, did not disappear after 14 days. Pyrethroid pesticide residues were detected in the urine samples of many consumers [14], as well as in agricultural producers in northern Thailand, and 3-phenoxybenzoic acid (a representative intermediate toxic product of pyrethroid) was also frequently detected in these samples [15].

Microbial bioremediation represents an effective strategy for the cleanup of contaminated environments, offering advantages such as low cost, a lack of secondary contamination, and ease of operation [16,17]. At present, several strains from different sources have been reported to effectively remove residual pyrethroids from the environment. The Gram-positive bacterium *Staphylococcus succinus* HLJ-10 can remove 90 % of D-cyphenothrin within 7 days [18]. Bhatt et al. [19] identified the bacterial strain *Sphingomonas trueperi* CW3, which can degrade more than 93 % of allethrin within 7 days. Recently, *Rhodococcus pyridinivorans* Y6 was found to rapidly remove prallethrin from the environment, and a prallethrin degradation enzyme, PnbA1564, was identified [20]. However, the molecular mechanisms underlying the microbial degradation of the widely used pyrethroid D-cyphenothrin have remained unclear.

Rhodococcus has emerged as one of the most promising microbial strains in biotechnology due to its super metabolic capability and environmental versatility as well as for its ability to degrade a variety of exogenous pollutants in soil/water environments [20–22]. However, little is known about the molecular insight into the catabolism of D-cyphenothrin in *Rhodococcus*. Therefore, the objectives of this study are: (1) to obtain efficient *Rhodococcus* strains capable of degrading D-cyphenothrin and other pyrethroid insecticides; (2) to elaborate the corresponding metabolites and metabolic pathways of D-cyphenothrin; (3) to identify the crucial enzymes involved in the breakdown mechanism; and (4) to unlock the catalytic mechanisms of the degradation enzymes. The discovery of an effective D-cyphenothrin degrading carboxylesterase fills a gap in the molecular basis of D-cyphenothrin biodegradation and provides a potential candidate for bioremediation applications.

2. Materials and methods

2.1. Reagents and media Components

The D-cyphenothrin (purity 98 %) used in this study was purchased from STORDSYNTHESIS, China. Other pyrethroid pesticides, including fenvalerate (91 %), allethrin (98 %), bifenthrin (96 %), prallethrin (95 %), deltamethrin (99 %), tetramethrin (99 %), permethrin (97 %), and beta-cypermethrin (95 %), were purchased from Macklin (Shanghai, China). The chromatographic acetonitrile and methanol required for the mobile phase of high-performance liquid chromatography were obtained from Fisher Scientific, USA. Any unspecified chemical reagents used were of ordinary analytical grade.

Appropriate amounts of technical grade pyrethroids were each weighed to 100 mL of acetone, according to the purity of the respective pyrethroids, resulting in a stock solution with a pesticide concentration of 10,000 mg/L.

The Luria–Bertani (LB) medium was composed of yeast extract (5 g), peptone (10 g), and NaCl (10 g) per liter. The constituents of the mineral salt medium (MSM) included $(NH_4)_2SO_4$ (2 g), KH_2PO_4 (1.5 g), $Na_2HPO_4{\cdot}12H_2O$ (1.5 g), $MgSO_4{\cdot}7H_2O$ (0.2 g), $CaCl_2{\cdot}2H_2O$ (0.001 g), and $FeSO_4{\cdot}7H_2O$ (0.0001 g) per liter of distilled water. For the preparation of solid media, 15–20 g of agar per liter was incorporated into the respective liquid medium. All media were sterilized through autoclaving at 121℃ for 20 min.

2.2. Isolation and Identification of pyrethroid-degrading bacteria

Activated sludge, from which to isolate pesticide degraders, was obtained from a chemical plant wastewater treatment tank in Guangdong Province, China (23.37120° N, 113.19509° E). About 5 g of activated sludge was added to 50 mL of MSM containing 50 mg/L of D-cyphenothrin using enrichment culture technology [20]. After the enrichment culture was incubated at 30℃ for 7 days in a constant-temperature incubator, the D-cyphenothrin concentration was doubled, to 100 mg/L, by transferring 10 % of the inoculum to fresh MSM [20]. In a similar manner, after the D-cyphenothrin concentration reached 800 mg/L, 20 μL of the suspension was spread evenly in solid MSM containing 100 mg/L of D-cyphenothrin via gradient dilution and incubated at 30℃ until single colonies grew.

Individual bacterial colonies with different morphologies were selected and sub-cultured twice on LB agar medium to purify single bacterial strains. Individual strains were grown overnight in 1 mL of liquid LB medium, centrifuged at 6,000 rpm for 2 min, washed twice with sterilized saline, and resuspended in 1 mL of MSM. The prepared bacterial broth was supplemented into an Erlenmeyer flask containing 50 mL of sterile MSM, and D-cyphenothrin stock solution was added to result in an initial concentration of 50 mg/L. All of the flasks were incubated, with shaking, at 30℃ in a thermostatic incubator for 7 days, after which the MSM samples were extracted using ethyl acetate. The degradation rate of D-cyphenothrin with each individual strain was quantitatively analyzed using HPLC (high-performance liquid chromatography) [23].

The genomic DNA of each isolate was obtained using a bacterial genomic DNA extraction kit purchased from TransGen Biotech, amplified through PCR production using a bacterial 16S rDNA universal primer set (27F/1492R) synthesized by RuiBiotech, China [24], and entrusted to Beijing Genomics Institution (BGI, China) for sequencing. Meanwhile, the morphologies and cell structures of the bacteria were further observed and described using optical microscopy (Olympus, Japan) and a High-Resolution Field Emission Scanning Electron Microscope (FESEM-FEI Verios 460L, USA).

2.3. Kinetic analysis of D-cyphenothrin degradation

Strain Y14 was isolated from the enrichment medium containing D-

cyphenothrin and further investigated to determine its optimal utilization for various pyrethroid substrates, including D-cyphenothrin, fenvalerate, allethrin, bifenthrin, prallethrin, deltamethrin, tetramethrin, permethrin, and beta-cypermethrin. The stock solutions of various pesticides were added to each MSM, to achieve a final concentration of 50 mg/L. Pre-cultured strain Y14 reached an optical density (OD_{600}) of 1.0 overnight and was centrifuged and washed twice with normal saline. The washed cells were then inoculated into flasks containing various pesticides. Cultivation was carried out at 30℃, with shaking at 200 rpm, for 6 days under dark conditions. The degradation rate of each pesticide with strain Y14 was quantified using HPLC analysis.

Based on the high metabolic activity of strain Y14 toward D-cyphenothrin, an in-depth study was conducted on the degradation kinetics of D-cyphenothrin with strain Y14. Samples were extracted at regular intervals of 24 h, with the final batch assayed via HPLC after 6 days. Following the same intervals, the growth of strain Y14 in MSM supplemented with D-cyphenothrin was continuously monitored using a UV–visible spectrophotometer (Shimadzu UV-2410, Japan). To establish a baseline for comparison, all experimental setups included control cultures that without bacterial inoculation. In this process, a first-order kinetic model (Supplementary Eq.1) was applied to calculate the kinetic parameters for the biodegradation of D-cyphenothrin with strain Y14 [25]. In addition, the theoretical half-life (Supplementary Eq.2) is the most intuitive parameter through which to describe D-cyphenothrin degradation with strain Y14 [20]. The detailed equations are provided in the Supplementary Materials.

2.4. Degradation of D-cyphenothrin at different concentrations

Different concentrations of D-cyphenothrin were found to significantly influence the biological tolerance and metabolic activity of strain Y14. For this study, the concentrations of D-cyphenothrin were set to 10, 25, 50, 100, 200, 300, 400, and 500 mg/L. The inoculum was prepared by centrifuging the culture to achieve an OD_{600} value of 1.0, and samples were taken every 24 h. D-cyphenothrin can be used as a carbon and energy source for the growth of strain Y14 in MSM, but the growth rate of strain Y14 was inhibited with increases in D-cyphenothrin concentration. Therefore, the Andrews equation (Supplementary Eq.3) was employed to fit the data and elucidate the degradation capacity of strain Y14 under different concentration conditions [26].

2.5. Optimization of conditions for D-cyphenothrin degradation

The Response Surface Methodology (RSM) was applied to optimize the key factors and their interactive effects on the degradation of D-cyphenothrin by strain Y14 [27]. The Box–Behnken design for RSM was implemented using Design Expert software. Preliminary single-factor experiments identified temperature, pH value, and inoculum amount as crucial factors affecting D-cyphenothrin metabolism by strain Y14. Table S1 details the ranges and central values of the three independent variables (temperature, pH, and inoculum amount) determined using the Box-Behnken design. The dependent variable measured was the degradation rate of 50 mg/L of D-cyphenothrin after a 6-day treatment with strain Y14. The Box–Behnken design consisted of 17 experimental runs in a randomized block design [28]. The results from these experiments were modeled using a response surface program to fit a quadratic polynomial equation (Supplementary Eq.4).

Strain Y14 was cultured in LB liquid medium for 24 h, after which the OD_{600} values were adjusted to 0.5, 1.0, and 1.5, and 1 mL of the bacterial broth was centrifuged to pellet the cells. The collected cells were then washed twice with normal saline and resuspended. The resuspended broth was transferred into separate flasks of MSM, each containing 50 mg/L of D-cyphenothrin at pH levels of 5, 7 and 9, which were then incubated at temperatures of 20℃, 30℃, and 40℃ for a period of 6 days. Following incubation, the residual concentration of D-cyphenothrin in each flask was quantitatively measured using HPLC.

2.6. Metabolic pathway of D-cyphenothrin by strain Y14 and product toxicity analysis

The metabolic pathway of D-cyphenothrin was concurrently investigated in the pursuit of elucidating the degradation kinetics of strain Y14. Samples containing 50 mg/L of D-cyphenothrin and treated with strain Y14 were collected at various incubation periods for qualitative analysis using Gas Chromatography–Mass Spectrometry (GC–MS, Agilent 6890 N/5975, USA). The GC–MS analytical method was described in a previous study [26]. The metabolites were identified by comparing the results with standard compounds listed in the National Institute of Standards and Technology (NIST) database library, taking into account both the retention times and structural characteristics of intermediate products.

The toxicity of D-cyphenothrin was initially evaluated using the Ecological Structure Activity Relationships (ECOSAR) Predictive Model to analyze both its acute and chronic toxicities. The logarithmic-transformed toxicity (lg*k*) values of the parent compound D-cyphenothrin and its downstream metabolites were compared as a preliminary basis for toxicity assessment. Subsequently, the model organism *Escherichia coli* DH5α was serially diluted and spotted onto LB agar plates containing 0.05 mM, 0.5 mM, and 5 mM concentrations of D-cyphenothrin and its downstream metabolites, respectively. The growth of bacterial colonies was observed as the final criterion for toxicity evaluation [28].

2.7. Degradation potential of strain Y14 in soil and effect of microbial community

Soil samples were collected from topsoil at a depth of 5–15 cm at 23°16′82″ N, 113°37′45″ E to assess pyrethroid degradation by strain Y14. This site had not been exposed to pyrethroid pesticides for over five years. The moisture content of the soil samples was maintained at approximately 30–40 %, and sieved through a 2 mm mesh. Both sterilized and unsterilized soil samples were prepared for simulated field remediation experiments. Sterilized soil was autoclaved at 121℃ for 120 min. Then, 250 g each of sterilized and unsterilized soil were transferred to 1000 mL flasks, each supplemented with the D-cyphenothrin stock solution to achieve a final concentration of 50 mg/L. The soil samples were further subjected to two treatments, inoculation and non-inoculation, with the inoculated samples receiving 5 mL of strain Y14 culture at an OD_{600} of 1.0. All experimental runs were performed in triplicate, with the uninoculated treatment serving as a control.

Total soil DNA was extracted using the E.Z.N.A.® Soil DNA Kit from OMEGA Bio-tek (Georgia, USA) in order to observe the community dynamics of candidate strain Y14 after its introduction into the soil. Soil samples were collected from inoculated, unsterilized soil at intervals of 1, 5, 9, 13, 17, 21, and 25 days and subsequently stored at −80℃ prior to the extraction of total DNA. The PCR amplification of soil genome was performed using primers 341F/805R [29]. The total reaction volume for PCR was 25 μL, consisting of 12.5 μL of Phusion Hot start flex 2X Master Mix, 2.5 μL of Forward/Reverse primers, and 50 ng of DNA template. The PCR products were purified by AMPure XT beads and sequenced by Illumina NovaSeq PE250. This sequencing process was facilitated by Hangzhou LC Biotechnology Co., Ltd.

2.8. Proteomic analysis of strain Y14

For proteomic analysis, *Rhodococcus ruber* strain Y14 was grown to the logarithmic phase and treated with D-cyphenothrin at a final concentration of 50 mg/L, while an equivalent volume of acetone was added to the control group. After 24 h of induction, the cultures were centrifuged at 4℃ to obtain cell pellets, which were ground in liquid nitrogen and mixed with appropriate volumes of 8 M urea and 1 % protease inhibitor, and then subjected to further disruption using ultrasonication, followed by centrifugation at 20,000 g and 4℃ for 20 min. The

proteomic sequencing and analysis were conducted with the assistance of Hangzhou LC Biotechnology Co., Ltd.

2.9. Screening and expression of D-cyphenothrin-degrading enzyme

Sequences of potential pyrethroid-degrading enzymes were obtained from the NCBI database and previous reports. All amino acid sequences of strain Y14 were aligned online in FASTA format for sequence similarity comparison. Several genes with high similarity based on proteomic data were selected to construct protein expression vectors. Following previous methods [20], the pET28b expression plasmid was digested with restriction enzymes *Xho*I and *Bam*H I (NEB, USA) to obtain linearized vectors. The genes from the Y14 genome were amplified with PCR using the high-fidelity enzyme 2 × Phanta®FlashMasterMix (Vazyme, China). Then, gene fragments were recombined with linearized vectors into circular protein expression vectors, the PCR primers for which are listed in Table S2.

The plasmids carrying the degrading enzyme genes were transferred into *Escherichia coli* DH5α competent cells (ToloBio, China) via a 70 s heat shock at 42℃. Subsequently, the plasmids were amplified in LB medium containing 100 mg/L of kanamycin, extracted, and similarly transformed into *E. coli* ArcticExpress (DE3) RP competent cells (Abbreviated RP) [30]. RP strains with the protein expression vector were cultured overnight, and isopropyl β-D-1-thiogalactopyranoside and D-cyphenothrin were added at final concentrations of 0.5 mM and 50 mg/L, respectively. Protein expression was then induced at 16℃ and 120 rpm, and the degradation of D-cyphenothrin was monitored at various time points.

2.10. Catalytic mechanism

The degrading enzyme amino acid sequence was uploaded to SWISS-MODEL (https://swissmodel.expasy.org) for sequence analysis, and the highest-matching protein crystal model was selected for homology modeling [31]. The quality of the constructed three-dimensional (3D) structure model of the degrading enzyme was assessed using the Ramachandran plot and the GMQE (Global Model Quality Estimate). Subsequently, molecular docking of the degrading enzyme with D-cyphenothrin was performed using AutoDockTools 1.5.7 and PyMOL 2.3.2 in a Python 2.5.4 environment [32]. Site-directed mutagenesis of the predicted active sites was carried out based on the results of the molecular docking using the Mut Express II Fast Mutagenesis Kit (Vazyme, China), and the activity of the mutated degrading enzyme was verified. The primers used for site-directed mutagenesis were listed in Table S2.

2.11. Statistical analysis

Origin 2019, Design-Expert, and GraphPad Prism software were utilized for the statistical analysis of the data obtained in this study. All of the results are presented as mean ± SD (standard deviation). Tukey's Honestly Significant Difference (HSD) test was employed, with a threshold of $p < 0.05$ set for indicating statistically significant differences between experimental groups.

3. Results

3.1. Isolation and Identification of degrading strains

In this study, 16 distinct colonies exhibiting varied morphologies were isolated from activated sludge using the enrichment culture technique. Notably, an isolate designated Y14 demonstrated a pronounced capacity for D-cyphenothrin removal. Following incubation on LB solid medium at 30 °C for 48 h, the colony of strain Y14 appeared pale red and opaque, with neat edges, a round shape, and a smooth surface, spanning approximately 1–3 mm in diameter (Fig. S1a). Gram staining confirmed the Gram-positive nature of strain Y14, and its cellular morphology was further elucidated using scanning electron microscopy (SEM), revealing cylindrical cells, approximately 1–3 μm in length and 0.6 μm in width, predominantly reproducing through division (Fig. S1b/c).

Phylogenetic analysis of the 16S rDNA genetic sequence showed that isolate Y14 belonged to genus *Rhodococcus* and had high similarity with *R. ruber* DSM 43338 (GenBank accession No. NR026185.1) (Fig. S1d). The 16S rDNA gene sequence of strain Y14 was uploaded to GenBank through online submission, and its accession number is MW485814. To further identify strain Y14 at the species level, multi-locus sequence typing (MLST) analysis was conducted on the evolutionary relationships of the *gapdh*, *tpi*, *mdh*, *icl*, *rpoC*, *recA*, and *adk* genes in the Y14 genome. The results showed that strain Y14 has the closest evolutionary relationship with the phenol-degrading strain *R. ruber* SD3 isolated from Nanchang, Jiangxi Province, China, and the weakest evolutionary relationship with *R. ruber* YC-YT1 isolated from seawater (Fig. S1e). Combining the 16S rDNA sequence analysis, MLST analysis and morphological characteristics, strain Y14 was conclusively identified as *Rhodococcus ruber*.

3.2. Kinetic analysis of D-cyphenothrin degradation

Strain Y14 was cultured in MSM supplemented with 50 mg/L of D-cyphenothrin, fenvalerate, allethrin, permethrin, prallethrin, tetramethrin, beta-cypermethrin, bifenthrin, and deltamethrin at 30℃ and 200 rpm for 6 days. D-cyphenothrin, allethrin, fenvalerate, prallethrin, and tetramethrin were completely removed with strain Y14. Subsequently, the degradation rates were ranked for beta-cypermethrin, bifenthrin, permethrin, and deltamethrin, corresponding to 94.13, 93.37, 83.64 and 66.07 % (Fig. 1).

The degradation process of D-cyphenothrin with strain Y14 were further analyzed, and the results are shown in Fig. 1a. D-cyphenothrin can be utilized by strain Y14 as a carbon source for growth. The degradation of D-cyphenothrin was positively correlated with the growth of strain Y14. Under the condition of using D-cyphenothrin as the sole carbon source, the growth of strain Y14 did not undergo an obvious lag phase, instead rapidly entering the logarithmic phase. The most rapid degradation of D-cyphenothrin occurred within the initial 48 h, and the degradation curve plateaued between 2 and 4 days as the strain reached a stable growth phase. After a 6-day incubation period, the degradation rate of D-cyphenothrin with strain Y14 achieved 100 %, significantly surpassing the mere 5.0 % for the natural degradation observed in the control group.

Table 1 shows the kinetic parameters of degradation for various pyrethroids with strain Y14 and demonstrates that the degradation process follows the first-order kinetic model. As shown in Table 1, the range of degradation constants for strain Y14 on various synthetic pyrethroids in the treated and control groups were 0.1774–0.8549 and 0.0277–0.1243, respectively. The theoretical half-life of the treatment group was significantly shorter than that of the control group, with ranges of 0.81–3.91 days and 5.58–25.02 days, respectively. The determination coefficients (R^2) for both the treatment and control groups were mostly greater than 0.8, indicating that the actual degradation data fit well with the first-order degradation kinetic model. These results further demonstrate that strain Y14 shows high potential for efficiently degrading pyrethroids.

3.3. Degradation of D-cyphenothrin at different concentrations

The efficacy of strain Y14 to degrade various concentrations of D-cyphenothrin is depicted in Fig. 2a. D-cyphenothrin was degraded most rapidly at a concentration of 25 mg/L, with strain Y14 exhibiting robust metabolic activity starting on the first day and achieving a degradation rate exceeding 75 %. Remarkably, concentrations of 10 mg/L and 25 mg/L were completely degraded by the fourth day, with no evident lag phase. After a 6-day cultivation period, strain Y14 was observed to

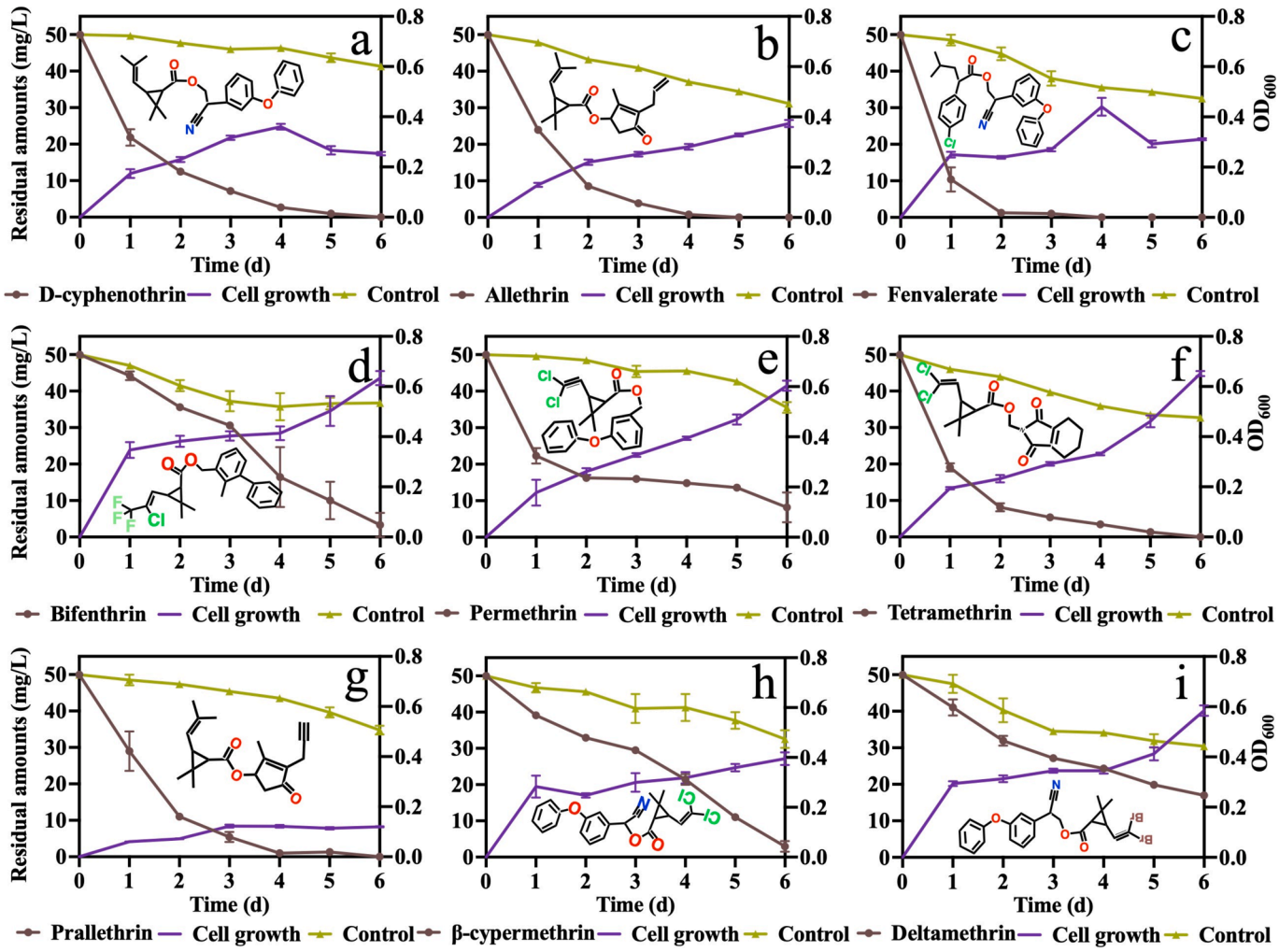

Fig. 1. Growth and degradation curves of multiple pyrethroid insecticides. a: D-cyphenothrin; b: allethrin; c: fenvalerate; d: bifenthrin; e: permethrin; f: tetramethrin; g: prallethrin; h: beta-cypermethrin; and i: deltamethrin.

degrade over 80 % of D-cyphenothrin, even at an elevated initial concentration of 500 mg/L. This finding underscores the capability of strain Y14 to maintain effective metabolic activity in environments heavily contaminated with D-cyphenothrin.

In this study, the Andrews equation was used to fit the metabolic process of strain Y14 for different concentrations of D-cyphenothrin. As shown in Fig. 2b, the Andrews model can fit both the theoretical and actual values of D-cyphenothrin degradation with strain Y14, and the correlation coefficient R^2 is 0.8303. When the concentration was 25 mg/L, the specific degradation rate (q_{max}) was the highest, at 0.9 d^{-1}. The half-rate constant (K_s) and inhibition coefficient (K_i) of the model were 2.0 mg/L and 221.9 mg/L, respectively. Based on K_i and K_s, the optimal substrate concentration for D-cyphenothrin metabolism by strain Y14 at the maximum specific degradation rate was 21.0 mg/L.

3.4. Optimization of conditions for D-cyphenothrin degradation

Design Expert software was used for testing according to the Box–Behnken design principle of response surface methodology, and the original results are shown in Table S3. The temperature (X_1), pH value (X_2), and inoculum (X_3) were selected as independent variables, and D-cyphenothrin residue was designated as the response value (Y_1), representing the dependent variable, for the derivation of a quadratic polynomial regression equation. Then, the three-dimensional response surface of strain Y14 degrading D-cyphenothrin was obtained using the equation. The extremum of the model was determined by calculating the first-order partial derivative of the equation and solving it to obtain the optimum conditions for the degradation of D-cyphenothrin with strain Y14. The derived quadratic polynomial regression equation for the degradation of D-cyphenothrin with strain Y14 is as follows:

$$Y_1 = 100.00 + 7.11X_1 + 8.79X_2 + 1.68X_3 + 7.42X_1X_2 - 1.50X_1X_3 + 0.25X_2X_3 - 11.96X_1^2 - 11.91X_2^2 - 1.09X_3^2.$$

The results of the statistical analysis showed that the quadratic polynomial regression equation could well evaluate the biodegradation process of D-cyphenothrin with strain Y14, with P value < 0.01. The single factors of temperature (X_1) and pH value (X_2) have significant effects on the degradation achieved with strain Y14 ($p < 0.05$), and the square terms X_1^2 and X_2^2 also reach significance for the degradation effects achieved with strain Y14; however, the model showed that the interaction terms of the three factors, namely X_1X_2, X_1X_3, and X_2X_3, had no significant effects on D-cyphenothrin degradation with strain Y14, as shown in Table S4 for variance analysis. The coefficient of determination R^2 of the model is 0.9005, and the low coefficient of variation (C.V. = 7.21 %) indicates that the prediction result of the model is acceptable, meaning that the predicted value of the model is basically consistent with the experimental value (Table S5).

The isothermal heat map presented in Fig. 3 suggests that the optimal metabolic capacity of strain Y14 for pH and temperature falls within the

Table 1
Kinetic parameters of degradation of various pyrethroids in mineral salt medium with treatment of strain Y14.

	Treatments	Regression equation	k (d^{-1})	R^2	$t_{1/2}$ (d)
D-cyphenothrin	Y14	$C_t = 50.36e^{-0.7550t}$	0.7550	0.9868	0.92
	Control	$C_t = 48.81e^{-0.0074t}$	0.0277	0.8134	25.02
Allethrin	Y14	$C_t = 49.56e^{-0.8549t}$	0.8549	0.9577	0.81
	Control	$C_t = 49.77e^{-0.0796t}$	0.0796	0.9928	8.71
Fenvalerate	Y14	$C_t = 48.27e^{-0.1164t}$	0.6987	0.7155	0.99
	Control	$C_t = 49.03e^{-0.0138t}$	0.0826	0.8944	8.39
Tetramethrin	Y14	$C_t = 47.91e^{-0.7091t}$	0.7091	0.9805	0.98
	Control	$C_t = 48.59e^{-0.0752t}$	0.0752	0.9833	9.22
Permethrin	Y14	$C_t = 51.50e^{-0.2326t}$	0.2326	0.8215	2.98
	Control	$C_t = 50.74e^{-0.0511t}$	0.0511	0.7955	13.56
Deltamethrin	Y14	$C_t = 48.30e^{-0.1774t}$	0.1774	0.9913	3.91
	Control	$C_t = 48.85e^{-0.1243t}$	0.1243	0.8906	5.58
Prallethrin	Y14	$C_t = 49.33e^{-0.7806t}$	0.7806	0.9697	0.89
	Control	$C_t = 47.16e^{-0.0752t}$	0.0752	0.9518	9.22
Bifenthrin	Y14	$C_t = 46.67e^{-0.4243t}$	0.4243	0.8804	1.63
	Control	$C_t = 45.55e^{-0.1106t}$	0.1106	0.9869	6.27
Beta-cypermethrin	Y14	$C_t = 49.20e^{-0.5992t}$	0.5992	0.6603	1.16
	Control	$C_t = 47.08e^{-0.1130t}$	0.1130	0.9129	6.13

Note: C_t refers to concentration of pyrethroids (mg/L); k refers to degradation rate constant; t refers to degradation times; R^2 refers to correlation coefficient.

coded value range of 0 to 1, while that of the inoculum dose had a wider coding value. Fig. 3b illustrates the interaction between pH and temperature during the degradation of D-cyphenothrin with strain Y14, indicating that strain Y14 exhibits maximal metabolic activity at a coded value of zero for both pH and temperature. As can be seen from Fig. 3bc, the contribution of inoculation amount to the degradation of D-cyphenothrin with strain Y14 was limited. Fig. S2 elucidates the individual effects of the three independent variables—temperature, pH value, and inoculum amount—on the degradation of D-cyphenothrin with strain Y14. Contrary to the results for temperature and pH value, the degradation rate did not significantly increase with higher inoculum amounts. This implies that effective pyrethroid remediation can be achieved with a relatively low concentration of strain Y14.

In order to obtain the optimal combination of degradation conditions for strain Y14, the first-order partial derivative of the quadratic polynomial regression equation was calculated, and the highest critical value of the model was acquired by solving the equation. Thus, the optimal degradation conditions for strain Y14 are as follows: a temperature of 32.77℃, a pH value of 8.09, and an inoculation amount of 1.15×10^7 CFU/mL. To verify the reliability of the analysis results, degradation tests were conducted under conditions before and after optimization. The results showed that after two days of incubation, the degradation rates were 75.05 % before optimization and 88.21 % after optimization, indicating a 13.16 % increase in degradation rate under the optimized conditions.

3.5. Metabolic pathway of D-cyphenothrin and product toxicity analysis

The intermediates produced during the metabolism of D-cyphenothrin by strain Y14 were identified using GC–MS. The analysis revealed two significant peaks at 27.97 and 28.05 min, both exhibiting identical characteristic mass spectral fragments at m/z 375. Based on comparisons with the National Institute of Standards and Technology database, the compound was identified as D-cyphenothrin. Concurrently with the degradation of D-cyphenothrin, four intermediate metabolites were detected at different time points (Fig. S3). The chemical structures, retention times (RTs), and molecular ion information of all metabolites are detailed in Table S6.

The comparison with the authoritative compounds in the National Institute of Standards and Technology (NIST) library database revealed the sequential appearance of D-cyphenothrin metabolites as chrysanthemic acid, 2-(3-hydroxyphenyl)acetonitrile, 3-phenoxybenzaldehyde and phenylmethanol (Fig. 4). The mass spectra of these D-cyphenothrin metabolites, which exhibited 90–100 % similarity with entries in the NIST library database. Based on the sequential detection of intermediate metabolites and the comparison results from the NIST library database, a biodegradation pathway for D-cyphenothrin metabolism by strain Y14 was proposed (Fig. 4e). Under the action of catabolic enzymes, D-cyphenothrin was first cleaved into chrysanthemic acid and α-hydroxy-3-phenoxy-benzeneacetonitrile through ester bond cleavage. α-Hydroxy-3-phenoxy-benzeneacetonitrile undergoes further dehydroxylation and dephenylation to form 2-(3-hydroxyphenyl) acetonitrile, which has negligible environmental toxicity. This compound is generally considered to be an intermediate for the synthesis of the heart disease drug Atenolol, which was first discovered in the biological metabolic pathway of pyrethroids. 2-(3-Hydroxyphenyl)

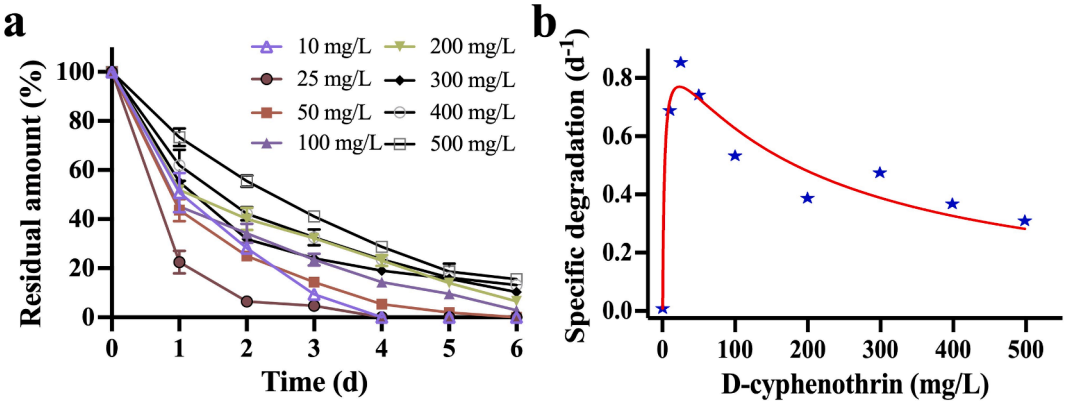

Fig. 2. Degradation characteristics of strain Y14 for different concentrations of D-cyphenothrin. a: Degradation curves of different concentrations of D-cyphenothrin metabolized by strain Y14. b: Inhibition curves of different concentrations of D-cyphenothrin degraded with strain Y14, fitted with the Andrews model.

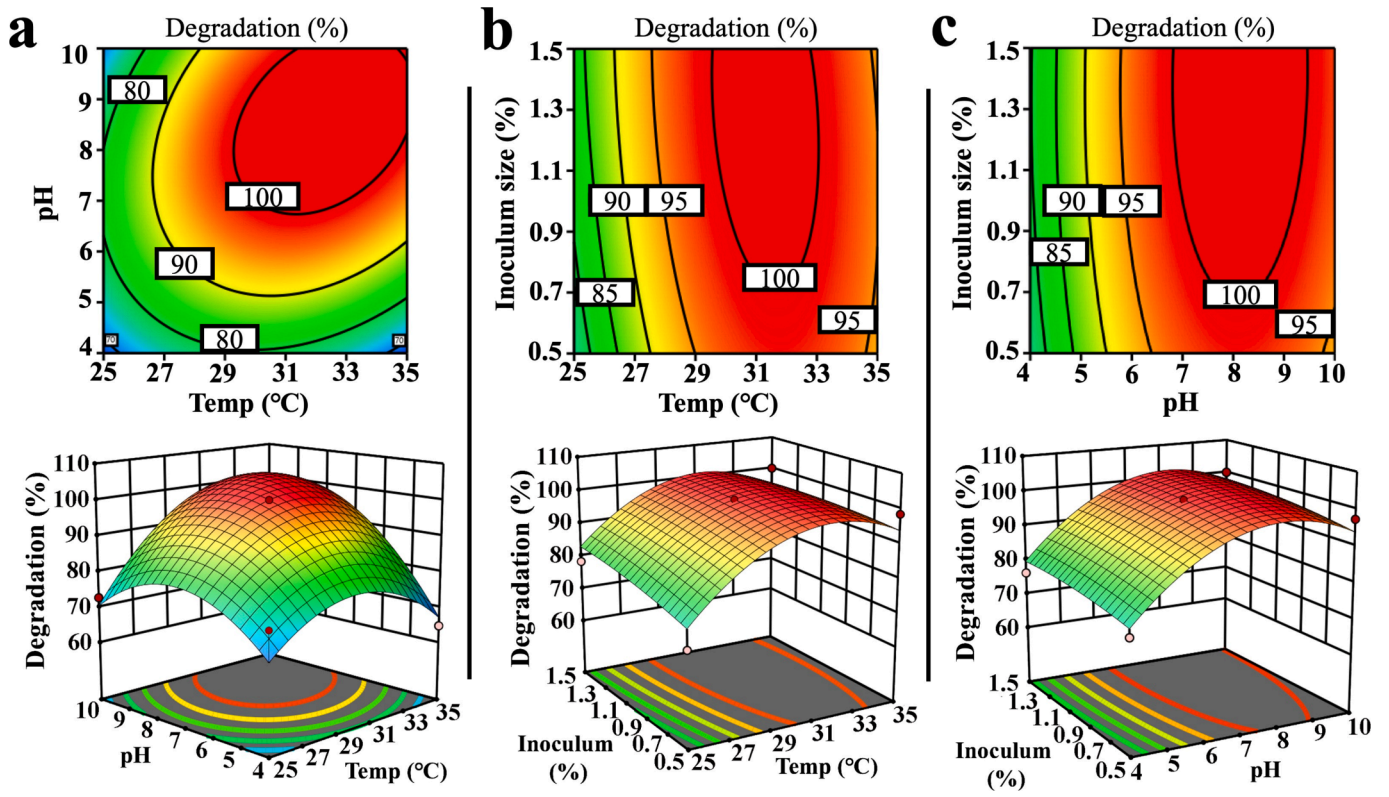

Fig. 3. Prediction of optimal degradation conditions based on response surface program. a: Interaction of pH and temperature on degradation capacity; b: interaction of inoculum amount and temperature on degradation capacity; and c: interaction of inoculum amount and pH on degradation capacity.

acetonitrile is then metabolized to phenol.

Concurrently, another metabolite of *α*-hydroxy-3-phenoxy-benzeneacetonitrile, 3-phenoxybenzaldehyde, is hydrolyzed into phenol and benzyl alcohol. On the other hand, following the initial hydrolysis of D-cyphenothrin into chrysanthemic acid and *α*-hydroxy-3-phenoxy-benzeneacetonitrile by strain Y14, the cyclopropane structure in chrysanthemic acid undergoes further decomposition and cleavage. This process results in the formation of smaller molecular compounds, which were not detected in this study.

The ECOSAR toxicity analysis revealed that the acute and chronic toxicity lg*k* values of D-cyphenothrin in fish, daphnids, and green algae ranged from −0.987 to −2.114, indicating that D-cyphenothrin is highly toxic to aquatic organisms (Fig. S4a). In contrast, the lg*k* values of chrysanthemic acid (M1) and *α*-hydroxy-3-phenoxy-benzeneacetonitrile (M2) ranged from 0.774 to 2.196, suggesting that these metabolites exhibit low toxicity. However, the lg*k* values of the metabolite 3-phenoxybenzaldehyde (M3), decreased to a range of 0.301 to 0.625, indicating a moderate level of toxicity. Further evaluation of the toxicity levels of the downstream metabolites of 3-phenoxybenzaldehyde (M3) showed that benzyl alcohol (M5) and phenol (M6) have lg*k* values ranging from 0.995 to 2.863, suggesting low or negligible toxicity. Notably, the novel intermediate identified in this study, 2-(3-hydroxyphenyl)acetonitrile (M4), exhibited the highest lg*k* values, indicating that this compound is non-toxic (Fig. S4a).

To validate the results of the ECOSAR toxicity analysis, 3-phenoxybenzaldehyde, which has a relatively high lg*k* value, was selected as a representative metabolite for comparison with the parent compound D-cyphenothrin in *E. coli* DH5*α* growth assay, as illustrated in Fig. S4b. The results demonstrated that at concentrations below 0.5 mM, *E. coli* DH5*α* grew well on LB agar plates containing either D-cyphenothrin or 3-phenoxybenzaldehyde. However, at a concentration of 5 mM, D-cyphenothrin completely inhibited the growth of *E. coli* DH5*α*, while 3-phenoxybenzaldehyde only slightly inhibited the growth of *E. coli* DH5*α*. These experimental findings were consistent with the prediction of the ECOSAR toxicity analysis, suggesting that the biodegradation of D-cyphenothrin was a detoxification process.

3.6. *Degradation potential of strain Y14 in soil and effect of microbial community*

Evaluating the biodegradation of D-cyphenothrin with strain Y14 under laboratory soil conditions is of great significance for studying the bioremediation potential of this strain in an actual field environment. Additionally, the interaction between strain Y14 and indigenous microorganisms played a key role in the metabolism of D-cyphenothrin. The results of simulated field experiments on strain Y14 are shown in Fig. 5a. A significant D-cyphenothrin elimination effect, exceeding 80 % after 25 days, was observed among different treatments, especially in the soil supplemented with strain Y14, including sterilized and unsterilized soil. Among them, the degradation rate of D-cyphenothrin in unsterilized soil was 92.45 %, significantly higher than the rate of 80.74 % for the sterilized soil treatment group. Similarly, in the control group without strain Y14, the unsterilized soil showed a higher natural degradation effect on D-cyphenothrin than the sterilized soil, with the highest natural degradation rate of 64.72 %.

The first-order kinetic behavior of strain Y14 in soil was further analyzed, and the results are listed in Table 2. The degradation rate constant of strain Y14 was higher than that of the uninoculated soil group. The highest degradation rate constant was 0.1001 d^{-1}, in unsterilized inoculated soil; the lowest was 0.0303 d^{-1}, in sterilized uninoculated soil. The theoretical half-life ($t_{1/2}$) values showed the advantage of strain Y14 more intuitively, as the $t_{1/2}$ of the unsterilized inoculation treatment group was only 6.9246 d, three times shorter than that of the sterilized control group, at 22.8761 d. The coefficients of determination (R^2) for the degradation kinetic models of all treatments were higher than 0.9, indicating that the first-order kinetic models were

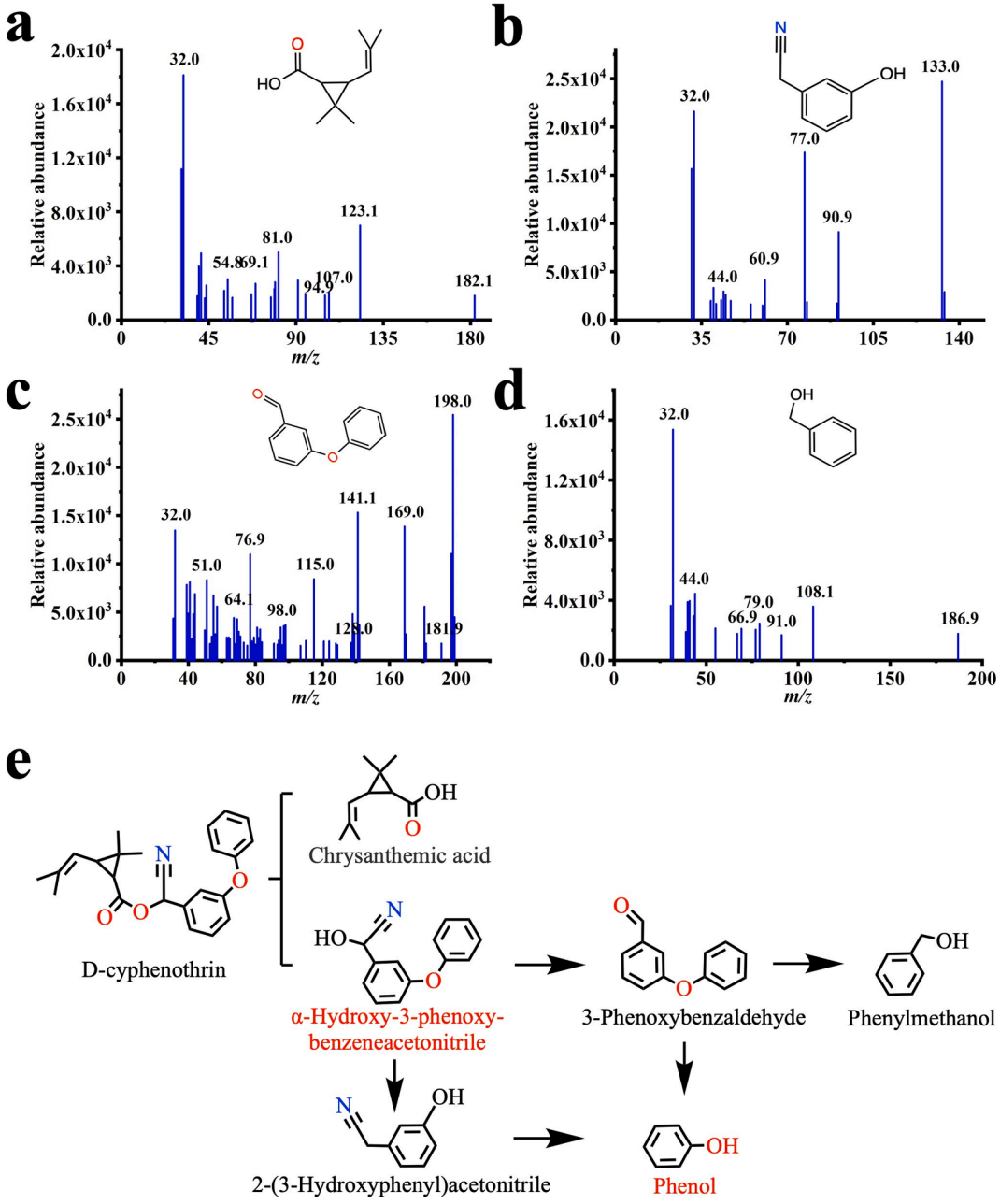

Fig. 4. Intermediate metabolites of D-cyphenothrin degraded with strain Y14 and possible metabolic pathways. a: Mass spectrum of chrysanthemic acid; b: mass spectrum of 2-(3-hydroxyphenyl)acetonitrile; c: mass spectrum of 3-phenoxybenzaldehyde; d: mass spectrum of phenylmethanol; and e: proposed degradation pathways of D-cyphenothrin with strain Y14. *NOTE*: The red font indicates that the intermediate is not detected with GC–MS. (For interpretation of the references to colour in this figure legend, the reader is referred to the web version of this article.)

well fitted to the process of D-cyphenothrin degradation with strain Y14. This demonstrates that the presence of indigenous microorganisms in unsterilized soil samples is beneficial for promoting the natural metabolism of D-cyphenothrin. Furthermore, it suggested that strain Y14 could not only degrade D-cyphenothrin rapidly in MSM, but also maintain efficient D-cyphenothrin metabolism in a complex soil environment.

In order to investigate the impact of strain Y14 on native soil ecology upon its introduction to the soil environment, high-throughput sequencing was employed to analyze shifts in bacterial community composition at different incubation stages, the results of which were used for bacterial diversity research after validity analysis. Table S7 illustrates the validity of samples at different culture periods. In alpha diversity analysis, the Chao1, Shannon, and Simpson indices are the most commonly used features for indicating species diversity and evenness. The results indicated a noticeable downward trend in both the Chao1 and Shannon indices within the first 9 days following the addition of strain Y14 (Fig. S5); however, these indices returned to their initial levels by the 25th day. Throughout the observation period, the Simpson index maintained its highest level, suggesting that the sudden introduction of strain Y14 did not adversely impact the community evenness of indigenous microorganisms.

The β-diversity analysis results highlighted significant shifts in the soil microbial community during the early stages of soil remediation with strain Y14. Proteobacteria and Actinobacteria emerged as the most dominant phyla, collectively comprising 63 % of the total identified species. They were followed by Acidobacteria and Chloroflexi, which accounted for 19 % of the total species. The relative abundance of

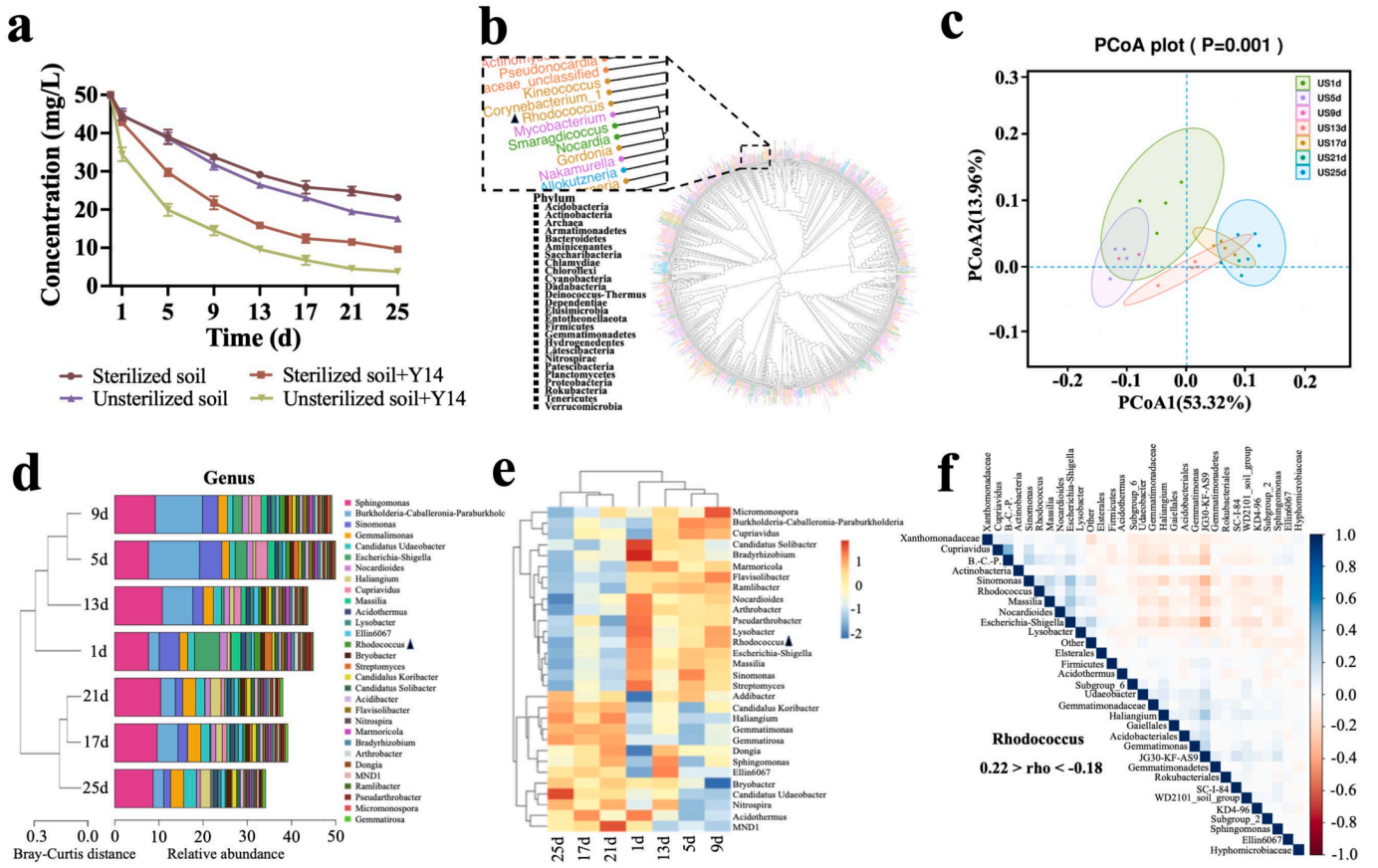

Fig. 5. Performance of strain Y14 in environmental applications. a: Degradation of D-cyphenothrin under different soil conditions; b: multiple sequence alignment of phylogenetic branches of soil samples; c: principal coordinates analysis (PCoA) of community composition of strain Y14 during soil remediation; d: stacked graph of microorganism abundance at different culture stages; e: cluster heatmap of changes in the abundance levels of microorganisms at different culture stages; and f: the correlation network heatmap between *Rhodococcus* and the dominant species among the indigenous microorganisms.

Table 2
Kinetic parameters of degradation of D-cyphenothrin in different soils by strain Y14.

Treatments	Regression equation	k (d^{-1})	R^2	$t_{1/2}$ (d)
SS	$C_t = 50.4241e^{-0.0303t}$	0.0303	0.9617	22.8761
US	$C_t = 51.0620e^{-0.0416t}$	0.0416	0.9919	16.6622
SS + Y14	$C_t = 51.7432e^{-0.0661t}$	0.0661	0.9641	10.4863
US + Y14	$C_t = 48.9707e^{-0.1001t}$	0.1001	0.9768	6.9246

Note: SS stands for sterilized soil; US stands for unsterilized soil.

Proteobacteria initially increased and subsequently decreased, while that of Actinobacteria exhibited a consistent downward trend, from 23.22 % to 13.02 %. In contrast, Acidobacteria and Chloroflexi both displayed increasing trends throughout the observation period. At the genus level, *Sphingomonas*, *Burkholderia–Caballeronia–Paraburkholderia*, *Sinomonas*, and *Escherichia–Shigella* were identified as the predominant genera in the early stages of the intervention (Table S8). Further analysis involved the multiple sequence alignment of the soil sequencing results, which revealed that *Rhodococcus*, within the Actinobacteria phylum, was evolutionarily closely related to *Mycobacterium*, *Gordonia*, *Nocardia*, and *Smaragdicoccus*, as shown in Fig. 5b.

The composition of the bacterial community changed significantly with the extension of incubation time. Principal coordinates analysis (PCoA) illustrated the extent of the differences in community composition between samples at different culture stages. As shown in Fig. 5c, there were significant differences in bacterial community structure between the two subgroups ($p = 0.001$). Anosim similarity analysis showed that there were differences among the seven groups of samples at different culture stages (1 d, 5 d, 9 d, 13 d, 17 d, 21 d, and 25 d; $R^2 = 0.7810$; $p = 0.001$). Similarly, NMDS (Nonmetric Multidimensional Scaling) also reflected the degree of difference between samples. As shown in Fig. S6, the stress value between samples is 0.07, indicating that it has excellent analytical significance. A cluster analysis based on Bray–Curtis distance demonstrated that the relative abundance levels of *Burkholderia–Caballeronia–Paraburkholderia* and *Cupriavidus* increased rapidly and then returned to their initial levels. Those of *Gemmatimonas* and *Haliangium* increased slowly, while those of most of the other genera showed significant downward trends (Fig. 5d).

The highest relative abundance of strain Y14 was observed on the first day after entering the soil, and it was maintained at a normal level for the following 9 days (Fig. S7). However, the abundance of *Rhodococcus* was observed to decline rapidly after 13 days of incubation, and it was eventually maintained at a low level. Cluster heatmaps were used to visualize changes in bacterial communities at different culture stages (Fig. 5e). During D-cyphenothrin degradation in soil, bacterial communities mainly clustered in two subgroups, with day 13 as the boundary. Notably, the genus *Rhodococcus* maintained high abundance levels within 9 days after incubation, suggesting that strain Y14 did not undergo a rapid or drastic adaptive process upon entry into the soil. The analysis results of the correlation network heatmap, illustrated in in Fig. 5f, demonstrate that the correlation coefficients (rho values) between *Rhodococcus* and other indigenous microorganisms range from 0.22 to −0.18, indicating that there is no correlation between the degradation behavior of strain Y14 and the dominant species among the indigenous microorganisms.

3.7. Proteomic analysis of strain Y14

The principal component analysis (PCA) plot for the protein samples in both the treatment and control groups is shown in Fig. 6a, and it indicates a high degree of aggregation among replicates, meeting the requirements for proteomic analysis. The standard deviation analysis between the treatment and control groups is presented in Fig. S8. In total, 3501 proteins were identified through comparison with the protein database, of which 3367 proteins were amenable to further quantitative analysis. Based on the ratio of protein relative expression in the experimental group compared to that in the control group, a quantitative value greater than 1.2 was considered upregulated, while a value less than 1/1.2 was considered downregulated. Among the 3367 quantified proteins, 506 were identified as upregulated, while 946 were downregulated. Specifically, there were 136 significantly upregulated and 452 significantly downregulated proteins (fold change, FC > 1.5) (Fig. 6b).

The most abundant among the 506 upregulated proteins were Uncharacterized Conserved Proteins (24), followed by Transcriptional Regulators (10) and Acetyltransferases (5). Of the 946 downregulated

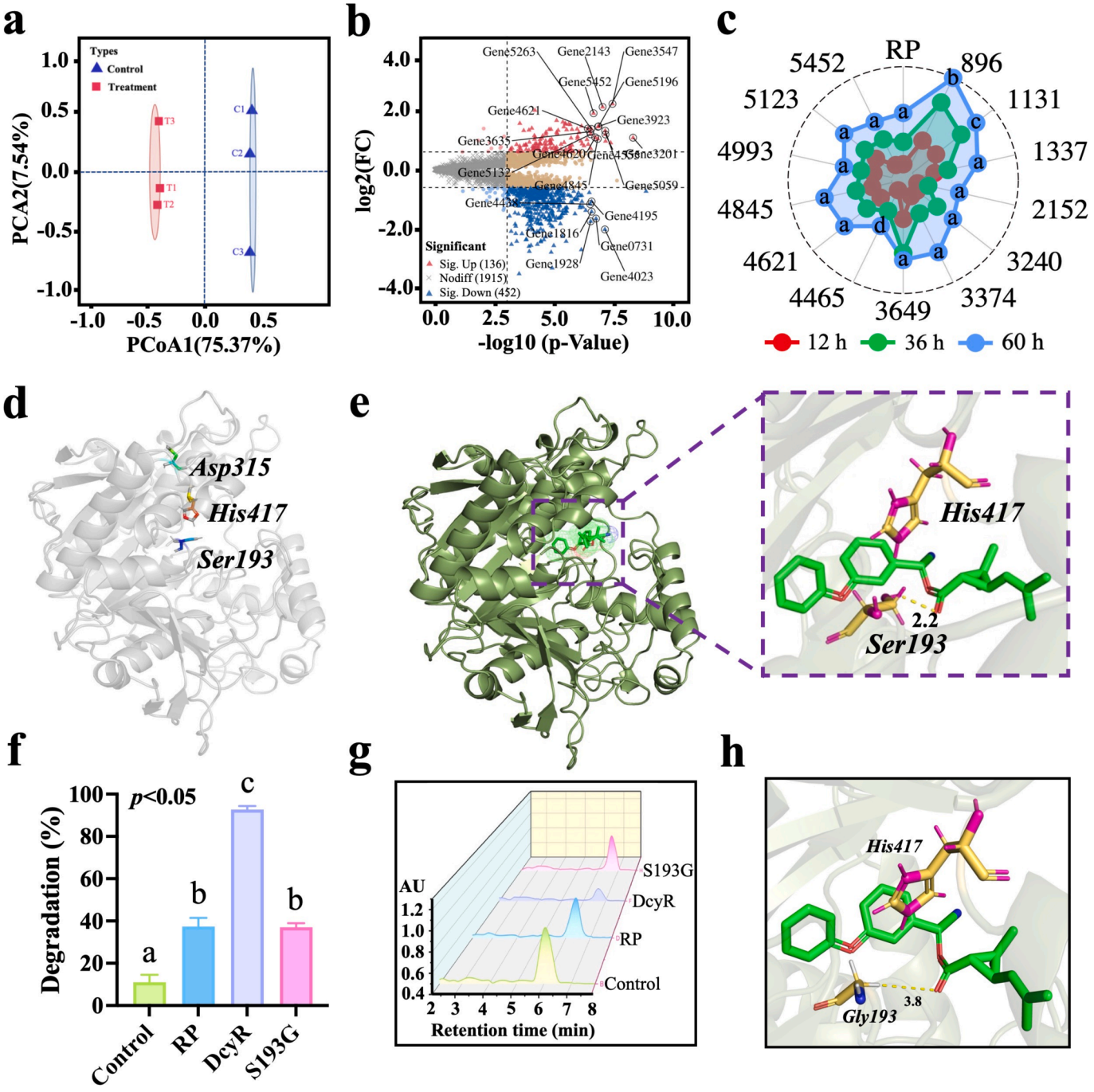

Fig. 6. Screening and mechanism analysis of D-cyphenothrin degrading enzymes. a: The principal component analysis (PCA) for the protein samples in both the treatment and control groups; b: the volcanic map of regulated proteins; and c: the metabolic potentials of different degrading enzymes; d: catalytic triad structure (Asp-Ser-His) of ORF896; e: molecular docking indicating that serine was the active site; f: Point mutation of Ser193 into glycine; g: degradation effects before and after point mutation; and h: comparison of peak area after point mutation. *NOTE*: Notation with identical letters indicates that there is no significant difference between the compared groups at the $p < 0.05$ level.

proteins, Uncharacterized Conserved Proteins were again the most common (41), followed by Acyl-CoA Dehydrogenases (27) and Dehydrogenases (25), suggesting a downregulation of proteins involved in the initial steps of fatty acid β-oxidation. Subcellular localization showed that 43.68 % and 15.22 % of upregulated proteins were located in the cytoplasm and cytoplasmic membrane, respectively (Fig. S9). Further analysis of the 48 most significantly upregulated proteins (FC > 2.0) revealed no upregulated gene clusters or esterase family proteins; however, the upregulation of ABC transporters was significant, with a fold increase of up to 4.493, and 5 ABC transporter-related proteins were among the 48 proteins. This suggests that, under the stress of D-cyphenothrin, strain Y14 may upregulate membrane transport proteins to facilitate the transport of D-cyphenothrin and its metabolites, thereby tolerating and resisting adverse environmental conditions.

Analysis using the COG (Clusters of Orthologous Groups of proteins) database revealed that proteins involved in 'Amino acid transport and metabolism' and 'Energy production and conversion' were the most upregulated, accounting for 51 and 48 proteins, respectively. The GO (Gene Ontology) database is primarily divided into three major categories: Biological Process (BP), Cellular Component (CC), and Molecular Function (MF). Upregulation was observed for 386, 270, and 191 proteins in these respective categories. Among these, the most significantly upregulated subsets were 'Thiamine-containing compound metabolic process' and 'Thiamine metabolic process' in the BP category; 'Oxidoreductase complex' in the CC category; and 'Oxidoreductase activity' in the MF category (Fig. S10). This indicates that proteins related to metabolic and redox processes are generally upregulated following induction from D-cyphenothrin, thus providing strong evidence that strain Y14 is capable of efficiently metabolizing a variety of synthetic pyrethroids.

Subsequently, the amino acid sequence of strain Y14 was compared with the amino acid sequences of other reported pyrethroid-degrading enzymes (Table S9). The results showed that the Y14 genome contains 21 proteins with similarities to those of reported pyrethroid-degrading enzymes, with the highest similarity being 41.82 %, and the lowest being 22.73 %. Among these 21 proteins, ORF796 (FC 1.229), ORF896 (FC 1.200), and ORF2496 (FC 1.343) were upregulated in the proteomics. Based on proteomic data, 35 genes were selected for constructing protein expression vectors, and 28 were successfully constructed. RP strains carrying different exogenous genes were divided into three batches for degradation testing, and ORF896 exhibited the highest degradation rate, achieving 92.73 % degradation after 60 h of induced expression. This was followed by ORF1131, with a degradation rate of 73.34 %. However, the control RP strain without exogenous genes also demonstrated a removal rate of approximately 38 % for D-cyphenothrin. Using the RP control as a benchmark, the degradation rates of proteins encoded by other genes ranged from −9.59 % to 14.13 %, and they did not show significant D-cyphenothrin removal rates at the $p < 0.05$ level (Fig. 6c). Therefore, ORF896 was further analyzed to determine its metabolic mechanism.

3.8. Degradation enzyme and its catalytic mechanism

Further research through the protein database revealed that ORF896 encodes a carboxylesterase family hydrolase composed of 513 amino acids, with a molecular weight of 55.92 kDa (Fig. S11a). The instability index of ORF896 is 33.71, indicating that the protein is stable. The isoelectric point of ORF896 is 5.46, the average hydropathicity value of its amino acids is −0.138, its aliphatic index is 84.09, and its molar extinction coefficient is 88,350 $M^{-1}cm^{-1}$. The 3D structural model of ORF896 was constructed using the SWISS-MODEL website, as depicted in Fig. S11b; the model's Ramachandran favored value reached 91.22 %, with a mere 0.19 % of amino acid residues falling in disallowed regions, significantly below the 10 % safety threshold. Additionally, the Global Model Quality Estimation (GMQE) value for this model was 0.70, surpassing the critical threshold of 0.5 and suggesting its suitability for advanced molecular docking analyses (Fig. S11c). Subsequently, multiple sequence conservation site analysis with carboxylesterases from various sources suggested that ORF896 possesses the classic pentapeptide motif (Gly-×-Ser-×-Gly) that is characteristic of carboxylesterases (Fig. S11d). Further examination of the enzyme's structure identified the presence of a typical catalytic triad (Asp315-Ser193-His417), a common feature in esterase enzymes (Fig. 6d).

The file of the D-cyphenothrin 3D model was obtained from the compound ligand website (https://zinc.docking.org). Subsequently, molecular docking was performed using the AutoDock software. The docking results are shown in Fig. 6e and indicate that Ser193 in ORF896 forms a hydrogen bond with the oxygen atom on the ester bond of D-cyphenothrin, with a bond length of 2.2 Å and a binding energy of −4.58 kcal/mol. To verify the reliability of the molecular docking results, Ser193 was site-specifically mutated to glycine. After validation with protein gel electrophoresis and sequencing, using the same induced expression and culturing for 60 h, it was observed that, compared to the control RP strain, ORF896-S193G lost its degradative activity for D-cyphenothrin (Fig. 6f). The peak area of D-cyphenothrin, when treated with the wild-type ORF896, was markedly lower than with the other three treatments, indicating higher degradation efficiency (Fig. 6g). In contrast, the natural degradation rate observed in the uninoculated control group was only 12.2 %. It can be seen from Fig. 6h that the spatial distance between Gly193 residue and D-cyphenothrin is too far (3.8 Å) to be conducive to the formation of hydrogen bonds. Therefore, the site-directed mutagenesis results strongly indicate that Ser193 is the key catalytic site in the carboxylesterase encoded by ORF896. Ultimately, the carboxylesterase encoded by ORF896 was named DcyR.

Fig. 7 illustrates that the DcyR hydrolysis mechanism of D-cyphenothrin is mediated through a catalytic triad, in which Ser193 serves as the nucleophile. Initially, D-cyphenothrin binds to DcyR, enabling the serine residue in the active site to conduct a nucleophilic attack on D-cyphenothrin's carbonyl group through its hydroxyl (OH) group, thus resulting in the formation of a tetrahedral intermediate I. The process then progresses to the second step, wherein the histidine residue from the catalytic triad dissociates from this intermediate, leading to the release of chrysanthemic acid and the formation of an acylated covalent intermediate. This is followed by the third step, in which the aspartic acid and histidine obtain protons from the hydroxyl group of the nucleophile, forcing the ester oxygen to accept electrons and forming another tetrahedral intermediate II.

Finally, the reduction of the carbonyl group in the intermediate II causes a proton transfer from histidine to serine, thus decomposing D-cyphenothrin into chrysanthemic acid and α-hydroxy-3-phenoxy-benzeneacetonitrile. During this catalytic process, the serine residue in the Asp-Ser-His catalytic triad acts as the nucleophile, the histidine residue acts as the proton donor, and the aspartic acid residue plays an assisting role. The dynamic schematic diagram of D-cyphenothrin within the strain Y14 cells is depicted in Fig. 8. Upon entry into strain Y14 cells, D-cyphenothrin induces cellular physiological stress responses, leading to elevated levels of superoxide dismutase (SOD), peroxidase (POD) and catalase (CAT) activities. Simultaneously, D-cyphenothrin is degraded by DcyR, forming catechol under the action of multiple oxidoreductases. Catechol then enters the pyruvate metabolism pathway under the help of catechol 1,2-dioxygenase and is ultimately degraded into pyruvate, which is integrated into the TCA cycle.

4. Discussion

Rhodococcus is an obligate aerobic, Gram-positive bacterium with high GC content and low motility, commonly found in soil and marine environments. Strains of the genus *Rhodococcus* have been reported to exhibit broad metabolic capabilities, capable of degrading a variety of compounds, including aliphatic and aromatic hydrocarbons, halogenated compounds, nitroaromatic hydrocarbons, and nitriles [33–36]. These versatile characteristics make them highly useful in

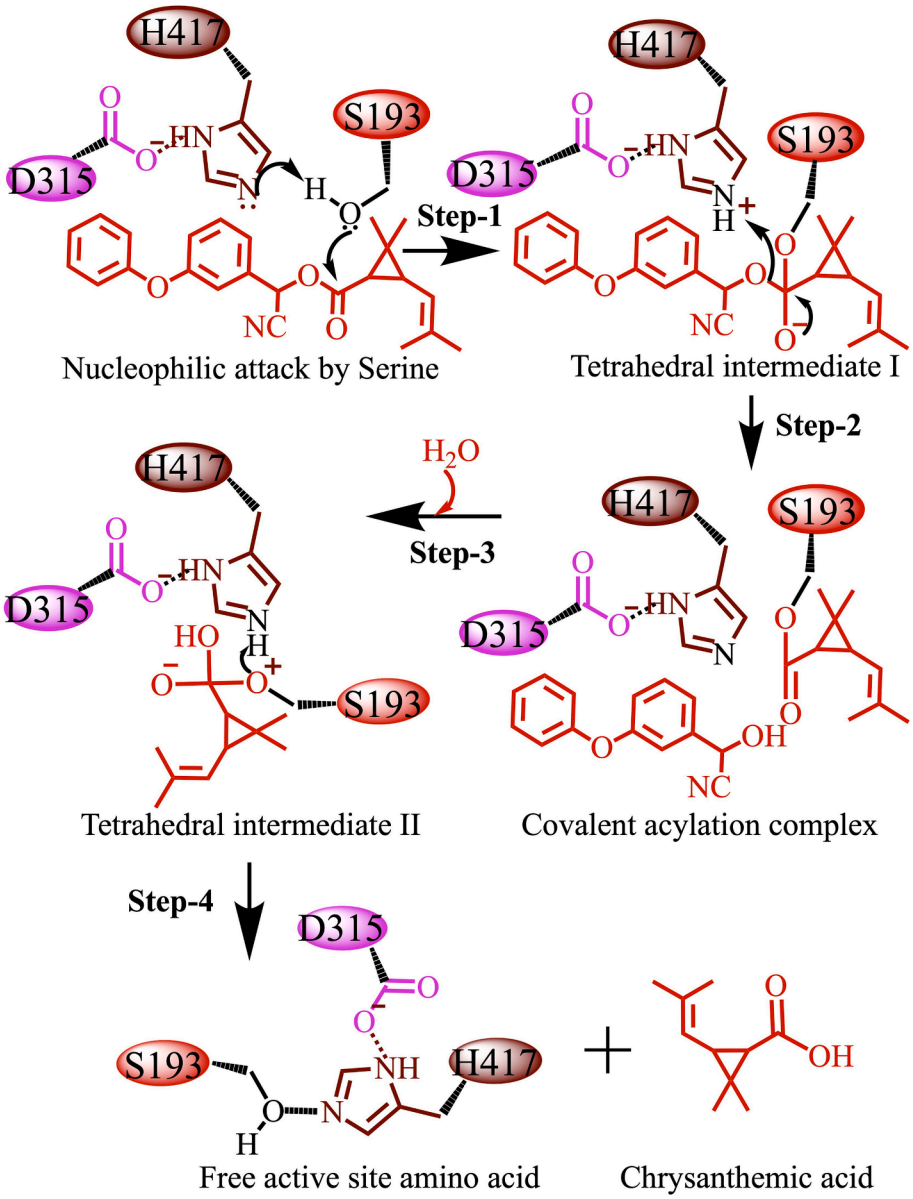

Fig. 7. Mechanism of catalytic triad decomposition of D-cyphenothrin.

environmental management, bioremediation, biosynthesis, and other industrial applications. It has been reported that *R. erythropolis* M−25 can effectively degrade crude oils, including an ability to synthesize biosurfactants that promote this degradation, achieving a degradation rate of 70.7 % after 30 days of treatment [37]. Furthermore, *R. ruber* DP-2 was capable of degrading di-n-butyl phthalate (DBP) and phenol efficiently. With an initial concentration range of 600–1,200 mg/L, the observed half-life of DBP was 15.81–27.75 h, and that of phenol was 14.52–45.52 h [38]. Additionally, polycyclic aromatic compounds, sulfonyl herbicides, anthraquinone compounds, and polychlorinated biphenyls have all been revealed to be eliminated by *Rhodococcus* from contaminated environments [36,39]. However, the molecular insights into the catabolism of D-cyphenothrin in *Rhodococcus* are largely unknown.

In this study, *R. ruber* Y14 was found highly effectively in degrading D-cyphenothrin and other widely used pyrethroids. The field of pyrethroid biodegradation has seen a plethora of advancements, with varying potentials exhibited by different microbial degraders [40–44]. Previous research has revealed that Gram-positive bacterium *Staphylococcus succinus* HLJ-10 can remove 90 % of D-cyphenothrin in 7 days; however, this strain demonstrates limited efficacy in degrading other types of pyrethroids [18]. *S. trueperi* CW3 can degrade over 93 % of allethrin within 7 days, while its degradation rate for D-cyphenothrin was 84 %, with a degradation rate constant (k) of 0.240 and a theoretical half-life of 2.88 days [19]. The half-life values are significantly higher than those observed with strain Y14, which has a theoretical half-life of 0.92 days for D-cyphenothrin degradation. In most cases reported to date, pure cultures isolated failed to remove synthetic pesticides from the natural environment [45–47]. It is noteworthy that bioaugmentation of D-cyphenothrin polluted soils with strain Y14 remarkably enhanced the disappearance rate of D-cyphenothrin. The proficiency of strain Y14 in degrading D-cyphenothrin and other pyrethroids in various environments is largely attributed to its super metabolic capability and environmental versatility.

Moreover, strain Y14 demonstrated efficient utilization of D-cyphenothrin as a nutrient substrate in MSM devoid of additional carbon sources, indicating its capacity to use D-cyphenothrin as the sole energy source for growth. While numerous bacteria capable of utilizing pyrethroid insecticides as their primary energy source exist, only a limited number of them achieve complete removal [20,44,48]. Prior studies

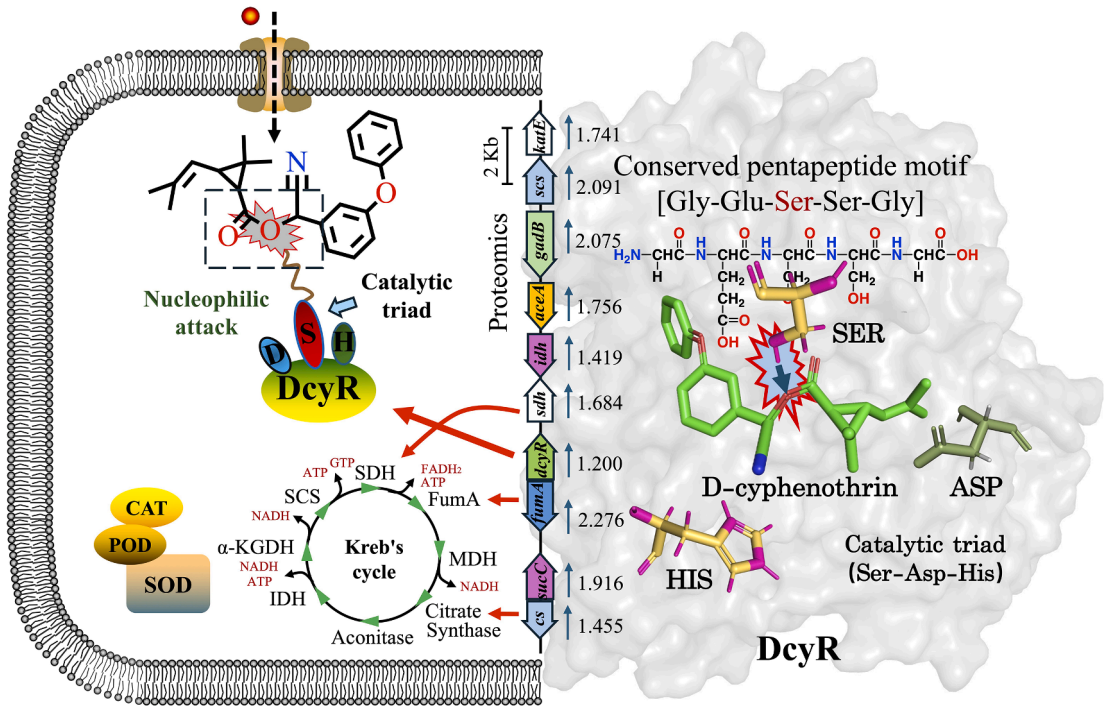

Fig. 8. The dynamic schematic diagram of D-cyphenothrin within the strain Y14 cells. *Note*: SOD refers to superoxide dismutase, POD refers to peroxidase, and CAT refers to catalase.

have shown that co-metabolism can significantly enhance the xenobiotic-degrading potential of microbes [49–51]. For instance, *Fusarium oxysporum* 2S3 and *Fusarium* sp. 4S4, isolated from agricultural soil, exhibited bioremediation rates of only 66 % and 70 %, respectively, for 100 mg/L of cypermethrin after 5 days in the absence of other nutrients. However, both of these rates increased to over 80 % with the addition of external carbon sources [52]. Chen et al. [53] identified a new pyrethroid-degrading bacterium, *Bacillus thuringiensis* ZS-19, which removed 100 % of cyhalothrin within 72 h, in minimal medium (MM) supplemented with glycerol and mannitol, additional carbon sources that are not present in MSM. Furthermore, Zhao et al. [49] demonstrated that substrates like glycerol, urea, and peptone could enhance the metabolism of beta-cypermethrin by *B. licheniformis* B-1. Recently, Khan et al. [50] found that the co-metabolism of *Fusarium equiseti* K3 and *Sphingobium* sp. S8 can effectively improve the removal of organochlorine pesticides in nutritionally deficient environments. These findings corroborate that strain Y14 can continue to effectively metabolize various pyrethroids in an auxotrophic environment.

The initial step in the degradation of pyrethroids usually involves the hydrolysis of the ester bond [54–59]. In this study, the reaction was catalyzed by carboxylesterase DcyR, which was capable of breaking down ester bonds to produce alcohol and acid derivatives. Although α-hydroxy-3-phenoxy-benzeneacetonitrile and phenol were not detected in this study, they have been documented in the literature as typical intermediates of type II pyrethroids [55]. Furthermore, α-hydroxy-3-phenoxy-benzeneacetonitrile was further transformed into 3-phenoxy-benzaldehyde and 2-(3-hydroxyphenyl)acetonitrile. Chrysanthemic acid is a common intermediate that represents the acid moiety in most pyrethroids. It has been reported that chrysanthemic acid, similar to α-hydroxy-3-phenoxy-benzeneacetonitrile, is an unstable intermediate [56]. The toxicological assessments indicated that the downstream metabolites of D-cyphenothrin exhibited significantly lower toxicity than the parent compound. These results revealed that the hydrolysis transformation process mitigated the toxic stress posed by D-cyphenothrin on both organisms and the environment.

The metabolic mechanism of strain Y14 toward pyrethroids is characterized by the enzyme-catalyzed cleavage of chemical bonds, followed by the systematic breakdown of the compound through various enzymatic reactions. The presence of synthetic pyrethroids can induce the expression of specific enzymes involved in their degradation [46,60–62]. In this study, proteomic results verified that strain Y14 has the ability to upregulate the genes encoding these enzymes in response to environmental pollutants, thus enhancing its capacity to metabolize a wide range of pyrethroid compounds. Specifically, the DcyR carboxylesterase identified from strain Y14, which contains a catalytic triad (D315-S193-H417), plays a crucial role in this process. These results aligned with the outcomes of prior studies that have characterized carboxylesterase enzymes in other microbial strains [60–63]. For instance, Zhai et al. [60] cloned and expressed a 25 kDa carboxylesterase PytZ with a typical catalytic triad (Ser105-Asp154-His185) from *Ochrobactrum anthropi* YZ-1, which can effectively remove pyrethroids at an optimal temperature and pH value of 35℃ and 7.5, respectively. Additionally, a 633 bp ORF carboxylesterase gene, *mse1*, was isolated from *Methylobacterium* sp. A-1 and has been shown to efficiently degrade cypermethrin [61]. This 22 kDa carboxylesterase possesses a catalytic triad (Ser106, Asp156, and His187) wherein the nucleophilic serine residue is located in the pentapeptide motif Gly-X-Ser-X-Gly. In our studies, molecular docking and site-directed mutagenesis further confirmed that the conserved Asp315, Ser193, and His47 residues are essential for protein function of DcyR. These findings unravel the degradation mechanism of D-cyphenothrin by *R. ruber* Y14 and lay a theoretical foundation for the better use of *Rhodococcus* species and their enzymes to remediate pyrethroid contamination.

Genome analysis further reveals that *R. ruber* strain Y14 contains numerous genes related to metabolism and degradation, including carboxylesterase genes, monooxygenase genes, dioxygenase genes, and cytochrome P450. The metabolic pathways most involved are benzoate metabolism and alkane metabolism. These findings suggest that the *Rhodococcus* species have evolved genetic adaptability, which endows them with the capability to degrade synthetic pyrethroids. These adaptations include the presence of genes encoding for esterases, hydrolases, and other enzymes involved in degradation pathways, as well as regulatory elements that control the expression of these genes in response to environmental stimuli. The degradation of pyrethroids with

R. ruber Y14 not only highlights the bacterium's role in bioremediation, but also provides insight into the metabolic versatility and adaptability of microbial life to organic contaminants. Understanding the specific enzymes and pathways involved can aid researchers in the development of biotechnological approaches to the detoxify and remove synthetic pyrethroids from the environment.

5. Conclusions

In summary, a novel Actinomycete strain, *R. ruber* Y14 can rapidly and efficiently remove D-cyphenothrin under extreme culture conditions and simulated field environments, and it exhibits broad-spectrum pyrethroid-metabolizing capability. Remarkably, this strain maintains over 80 % degradation efficiency for D-cyphenothrin concentrations as high as 500 mg/L. Soil remediation experiments indicate that the natural attenuation of D-cyphenothrin in unsterilized soil is significantly higher than that in sterilized soil. Further high-throughput soil sequencing reveals that strain Y14 can quickly adapt to soil conditions upon introduction, and indigenous microorganisms can accelerate the half-life of D-cyphenothrin in the soil environment. These findings suggest that strain Y14 is an ideal microbial degrader, suitable for the bioremediation of environments contaminated with D-cyphenothrin. Moreover, an analysis of its metabolic pathways and detoxification mechanisms shows that carboxylesterase DcyR decomposes D-cyphenothrin into non-toxic or low-toxicity chrysanthemic acid and α-hydroxy-3-phenoxy-benzeneacetonitrile through a nucleophilic attack on its carbonyl group. However, further in depth studies based on genetics and molecular biology are required to validate DcyR's role in the evolution of novel catabolic pathways and the degradation mechanisms of pyrethroid insecticides.

Ethical approval

This article does not contain any studies with human participants or animals performed by any of the authors.

CRediT authorship contribution statement

Yaohua Huang: Writing – original draft, Software, Resources, Methodology, Formal analysis, Data curation. **Shunkang Zhou:** Writing – review & editing, Methodology. **Wen-Juan Chen:** Writing – review & editing. **Xiaofan Zhou:** Writing – review & editing, Formal analysis, Data curation. **Shao-Fang Chen:** Writing – review & editing. **Haoran Song:** Writing – review & editing. **Zhenchen Yan:** Writing – review & editing. **Sandhya Mishra:** Writing – review & editing. **Mohamed A. Ghorab:** Writing – review & editing. **Pankaj Bhatt:** Writing – review & editing. **Shaohua Chen:** Writing – review & editing, Supervision, Project administration, Investigation, Funding acquisition, Conceptualization.

Declaration of competing interest

The authors declare that they have no known competing financial interests or personal relationships that could have appeared to influence the work reported in this paper.

Acknowledgements

This study was financially supported by grants from the National Natural Science Foundation of China (32470116), the Natural Science Foundation of Guangdong Province, China (2023A1515012552), Guangzhou Basic and Applied Basic Research Project, China (2024A04J6583), and the Postdoctoral Fellowship Program of CPSF, China (GZC20240510).

Appendix A. Supplementary data

Supplementary data to this article can be found online at https://doi.org/10.1016/j.cej.2025.160030.

Data availability

Data will be made available on request.

References

[1] J. Zhao, Y. Jiang, L. Gong, X. Chen, Q. Xie, Y. Jin, J. Du, S. Wang, G. Liu, Mechanism of β-cypermethrin metabolism by *Bacillus cereus* GW-01, Chem. Eng. J. 430 (2022) 132961.
[2] T.Y. Zhao, K.D. Hu, J.L. Li, Y.T. Zhu, A.P. Liu, K. Yao, S.L. Liu, Current insights into the microbial degradation for pyrethroids: strain safety, biochemical pathway, and genetic engineering, Chemosphere 279 (2021) 130542.
[3] Q. Lu, K. Pan, J. Liu, T. Zhang, L. Yang, X. Yi, G. Zhong, Quorum sensing system effectively enhances DegU-mediated degradation of pyrethroids by *Bacillus subtilis*, J. Hazard. Mater. 455 (2023) 131586.
[4] B. Liu, W. Wang, J. Qiu, X. Huang, S. Qiu, Y. Bao, S. Xu, L. Ruan, T. Ran, J. He, Crystal structures of herbicide-detoxifying esterase reveal a lid loop affecting substrate binding and activity, Nat. Commun. 14 (2023) 4343.
[5] H. Zhan, Y. Huang, Z. Lin, P. Bhatt, S. Chen, New insights into the microbial degradation and catalytic mechanism of synthetic pyrethroids, Environ. Res. 182 (2020) 109138.
[6] N. Barco-Bonilla, R. Romero-Gonzalez, P. Plaza-Bolanos, A. Garrido Frenich, J. L. Martinez Vidal, Analysis and study of the distribution of polar and non-polar pesticides in wastewater effluents from modern and conventional treatments, J. Chromatogr. A 1217 (2010) 7817–7825.
[7] Z. Chishti, S. Hussain, K.R. Arshad, A. Khalid, M. Arshad, Microbial degradation of chlorpyrifos in liquid media and soil, J. Environ. Manage. 114 (2013) 372–380.
[8] S. Mishra, Y. Huang, J. Li, X. Wu, Z. Zhou, Q. Lei, P. Bhatt, S. Chen, Biofilm-mediated bioremediation is a powerful tool for the removal of environmental pollutants, Chemosphere 294 (2022) 133609.
[9] W.X. Tang, D. Wang, J.Q. Wang, Z.W. Wu, L.Y. Li, M.L. Huang, S.H. Xu, D.Y. Yan, Pyrethroid pesticide residues in the global environment: an overview, Chemosphere 191 (2018) 990–1007.
[10] R.W. Holmes, B.S. Anderson, B.M. Phillips, J.W. Hunt, D.B. Crane, A. Mekebri, V. Connor, Statewide investigation of the role of pyrethroid pesticides in sediment toxicity in California's urban waterways, Environ. Sci. Technol. 42 (2008) 7003–7009.
[11] L. Delgado-Moreno, K. Lin, R. Veiga-Nascimento, J. Gan, Occurrence and toxicity of three classes of insecticides in water and sediment in two Southern California coastal watersheds, J. Agric. Food Chem. 59 (2011) 9448–9456.
[12] X. Liu, Y. Zhan, Y. Luo, M. Zhang, S. Geng, J. Xu, Almond organophosphate and pyrethroid use in the San Joaquin Valley and their associated environmental risk, J. Soils Sediments 12 (2012) 1066–1078.
[13] R. Djouaka, M.F. Soglo, M.O. Kusimo, R. Adeoti, A. Talom, F. Zeukeng, A. Paraiso, V. Afari-Sefa, M.G. Saethre, V. Manyong, et al., The rapid degradation of lambda-cyhalothrin makes treated vegetables relatively safe for consumption, Int. J. Environ. Res. Public Health 15 (2018) 1536.
[14] C.J. Burns, T.P. Pastoor, Pyrethroid epidemiology: a quality-based review, Crit. Rev. Toxicol. 48 (2018) 297–311.
[15] S. Hongsibsong, T. Prapamontol, J.X. Dong, C.S. Bever, Z.L. Xu, S.J. Gee, B. D. Hammock, Exposure of consumers and farmers to organophosphate and synthetic pyrethroid insecticides in Northern Thailand, J. Consum. Prot. Food. S 14 (2019) 17–23.
[16] P. Bhatt, X. Zhou, Y. Huang, W. Zhang, S. Chen, Characterization of the role of esterases in the biodegradation of organophosphate, carbamate, and pyrethroid pesticides, J. Hazard. Mater. 411 (2021) 125026.
[17] M. Cycoń, A. Mrozik, Z. Piotrowska-Seget, Bioaugmentation as a strategy for the remediation of pesticide-polluted soil: a review, Chemosphere 172 (2017) 52–71.
[18] Y.H. Huang, Z.Q. Lin, W.P. Zhang, S.M. Pang, P. Bhatt, E.R. Rene, A.J. Kumar, S. H. Chen, New insights into the microbial degradation of D-cyphenothrin in contaminated water/soil environments, Microorganisms 8 (2020) 473.
[19] P. Bhatt, Y. Huang, E.R. Rene, A.J. Kumar, S. Chen, Mechanism of allethrin biodegradation by a newly isolated *Sphingomonas trueperi* strain CW3 from wastewater sludge, Bioresour. Technol. 305 (2020) 123074.
[20] Y. Huang, S.F. Chen, W.J. Chen, X. Zhu, S. Mishra, P. Bhatt, S. Chen, Efficient biodegradation of multiple pyrethroid pesticides by *Rhodococcus pyridinivorans* strain Y6 and its degradation mechanism, Chem. Eng. J. 469 (2023) 143863.
[21] M. Cycoń, A. Zmijowska, Z. Piotrowska-Seget, Enhancement of deltamethrin degradation by soil bioaugmentation with two different strains of *Serratia marcescens*, Int. J. Environ. Sci. Technol. 11 (2014) 1305–1316.
[22] T.I. Gorbunova, D.O. Egorova, M.G. Pervova, T.D. Kyrianova, V.A. Demakov, V. I. Saloutin, O.N. Chupakhin, Biodegradation of trichlorobiphenyls and their hydroxylated derivatives by *Rhodococcus*-strains, J. Hazard. Mater. 409 (2020) 124471.
[23] S. Chen, Q. Lin, Y. Xiao, Y. Deng, C. Chang, G. Zhong, M. Hu, L.H. Zhang, Monooxygenase, a novel beta-cypermethrin degrading enzyme from *Streptomyces* sp, PLoS One 8 (2013) e75450.

[24] K.L. Cross, J.H. Campbell, M. Balachandran, A.G. Campbell, C.J. Cooper, A. Griffen, M. Heaton, S. Joshi, D. Klingeman, E. Leys, Z. Yang, J.M. Parks, M. Podar, Targeted isolation and cultivation of uncultivated bacteria by reverse genomics, Nat. Biotechnol. 37 (2019) 1314–1321.
[25] V. Fauvelle, M. Garel, C. Tamburini, D. Nerini, J. Castro-Jimenez, N. Schmidt, A. Paluselli, A. Fahs, L. Papillon, A.M. Booth, R. Sempere, Organic additive release from plastic to seawater is lower under deep-sea conditions, Nat. Commun. 12 (2021) 4426.
[26] Y. Huang, W.J. Chen, J. Li, M.A. Ghorab, N. Alansary, D.E. El-Hefny, G.S. El-Sayyad, S. Mishra, X. Zhang, P. Bhatt, et al., Novel mechanism and degradation kinetics of allethrin using *Bacillus megaterium* strain HLJ7 in contaminated soil/water environments, Environ. Res. 214 (2022) 113940.
[27] M.A. El-Bendary, S.S. Afifi, M.E. Moharam, M.M.A. Elsoud, N.A. Gawdat, Optimization of *Bacillus subtilis* NRC1 growth conditions using response surface methodology for sustainable biosynthesis of gold nanoparticles, Sci. Rep. 12 (2022) 20882.
[28] H. Song, W.J. Chen, S.F. Chen, M. Liu, G. Si, X. Zhu, K. Bhatt, S. Mishra, M. A. Ghorab, S. Chen, Unveiling the hydrolase Oph2876 mediated chlorpyrifos degradation mechanism in *Pseudomonas nitroreducens* and its potential for environmental bioremediation, J. Hazard. Mater. 483 (2025) 136570.
[29] J.B. Logue, C.A. Stedmon, A.M. Kellerman, N.J. Nielsen, A.F. Andersson, H. Laudon, E.S. Lindstrom, E.S. Kritzberg, Experimental insights into the importance of aquatic bacterial community composition to the degradation of dissolved organic matter, ISME J. 10 (2016) 533–545.
[30] M. Ferrer, T.N. Chernikova, M.M. Yakimov, P.N. Golyshin, K.N. Timmis, Chaperonins govern growth of Escherichia coli at low temperatures, Nat. Biotechnol. 21 (2003) 1266–1267.
[31] L. Bordoli, F. Kiefer, K. Arnold, P. Benkert, J. Battey, T. Schwede, Protein structure homology modeling using SWISS-MODEL workspace, Nat. Protoc. 4 (2009) 1–13.
[32] S. Forli, R. Huey, M.E. Pique, M.F. Sanner, D.S. Goodsell, A.J. Olson, Computational protein-ligand docking and virtual drug screening with the AutoDock suite, Nat. Protoc. 11 (2016) 905–919.
[33] B.S. Kant, G. Ranjit, C. Yong-Keun, L. Hong-Ju, K.S. Hyun, S.M. Ju, C.J. Yeon, H. Sion, L.S. Ho, C. Kwon-Young, et al., *Rhodococcus* sp. YHY01 a microbial cell factory for the valorization of waste cooking oil into lipids a feedstock for biodiesel production, Fuel 301 (2021) 121070.
[34] T. Zhao, Y. Gao, T. Yu, Y. Zhang, Z. Zhang, L. Zhang, L. Zhang, Biodegradation of phenol by a highly tolerant strain *Rhodococcus ruber* C1: biochemical characterization and comparative genome analysis, Ecotoxicol. Environ. Saf. 208 (2021) 111709.
[35] P. Wu, Y.S. Wang, Fluorene degradation by *Rhodococcus* sp. A2-3 isolated from hydrocarbon contaminated sediment of the Pearl River estuary, China, Ecotoxicology 30 (2021) 929–935.
[36] Z. Ye, H. Li, Y. Jia, J. Fan, J. Wan, L. Guo, X. Su, Y. Zhang, W.M. Wu, C. Shen, Supplementing resuscitation-promoting factor (Rpf) enhanced biodegradation of polychlorinated biphenyls (PCBs) by *Rhodococcus biphenylivorans* strain TG9(T), Environ. Pollut. 263 (2020) 114488.
[37] Y. Pi, B. Chen, M. Bao, F. Fan, Q. Cai, L. Ze, B. Zhang, Microbial degradation of four crude oil by biosurfactant producing strain *Rhodococcus* sp, Bioresour. Technol. 232 (2017) 263–269.
[38] Z. He, C. Niu, Z. Lu, Individual or synchronous biodegradation of di-n-butyl phthalate and phenol by *Rhodococcus ruber* strain DP-2, J. Hazard. Mater. 273 (2014) 104–109.
[39] H. Lu, X. Wang, M. Zang, J. Zhou, J. Wang, W. Guo, Degradation pathways and kinetics of anthraquinone compounds along with nitrate removal by a newly isolated *Rhodococcus pyridinivorans* GF3 under aerobic conditions, Bioresour. Technol. 285 (2019) 121336.
[40] W.G. Birolli, M.S. Arai, M. Nitschke, A.L.M. Porto, The pyrethroid (+/-)-lambda-cyhalothrin enantioselective biodegradation by a bacterial consortium, Pestic. Biochem. Physiol. 156 (2019) 129–137.
[41] H. Li, Y. Ma, T. Yao, L. Ma, J. Zhang, C. Li, Biodegradation pathway and detoxification of beta-cyfluthrin by the bacterial consortium and its bacterial community structure, J. Agric. Food Chem. 70 (2022) 7626–7635.
[42] X. Wu, C. Zhang, H. An, M. Li, X. Pan, F. Dong, Y. Zheng, Biological removal of deltamethrin in contaminated water, soils and vegetables by *Stenotrophomonas maltophilia* XQ08, Chemosphere 279 (2021) 130622.
[43] P. Bhatt, E.R. Rene, Y. Huang, X. Wu, Z. Zhou, J. Li, A.J. Kumar, A. Sharma, S. Chen, Indigenous bacterial consortium-mediated cypermethrin degradation in the presence of organic amendments and *Zea mays* plants, Environ, Res. 212 (2022) 113137.
[44] Y. Xiao, S.H. Chen, Y.Q. Gao, W. Hu, M.Y. Hu, G.H. Zhong, Isolation of a novel beta-cypermethrin degrading strain *Bacillus subtilis* BSF01 and its biodegradation pathway, Appl. Microbiol. Biotechnol. 99 (2015) 2849–2859.
[45] W.G. Birolli, B. Vacondio, N. Alvarenga, M.H.R. Seleghim, A.L.M. Porto, Enantioselective biodegradation of the pyrethroid (+/-)-lambda-cyhalothrin by marine-derived fungi, Chemosphere 197 (2018) 651–660.
[46] P. Bhatt, E.R. Rene, A.J. Kumar, W. Zhang, S. Chen, Binding interaction of allethrin with esterase: bioremediation potential and mechanism, Bioresour. Technol. 315 (2020) 123845.
[47] J. He, K. Zhang, L. Wang, Y. Du, Y. Yang, C. Yuan, Highly efficient degradation of cypermethrin by a co-culture of *Rhodococcus* sp. JQ-L and *Comamonas* sp. A-3, Front. Microbiol. 13 (2022) 1003820.
[48] W.J. Chen, W.P. Zhang, Q.Q. Lei, S.F. Chen, Y.H. Huang, B. Kalpana, L.S. Liao, X. F. Zhou, *Pseudomonas aeruginosa* based concurrent degradation of beta-cypermethrin and metabolite 3-phenoxybenzaldehyde, and its bioremediation efficacy in contaminated soils, Environ. Res. 236 (2023) 116619.
[49] J. Zhao, D. Jia, J. Du, Y. Chi, K. Yao, Substrate regulation on co-metabolic degradation of beta-cypermethrin by *Bacillus licheniformis* B-1, AMB Express 9 (2019) 83.
[50] N. Khan, E. Muge, F.J. Mulaa, B. Wamalwa, M. von Bergen, N. Jehmlich, L.Y. Wick, Mycelial nutrient transfer promotes bacterial co-metabolic organochlorine pesticide degradation in nutrient-deprived environments, ISME J. 17 (2023) 570–578.
[51] W.G. Birolli, B.F. da Silva, E. Rodrigues Filho, Biodegradation of the pyrethroid cypermethrin by bacterial consortia collected from orange crops, Environ. Res. 215 (2022) 114388.
[52] P. Kaur, A. Sharma, L. Parihar, In vitro study of mycoremediation of cypermethrin-contaminated soils in different regions of Punjab, Ann. Microbiol. 65 (2015) 1949–1959.
[53] S. Chen, Y. Deng, C. Chang, J. Lee, Y. Cheng, Z. Cui, J. Zhou, F. He, M. Hu, L. H. Zhang, Pathway and kinetics of cyhalothrin biodegradation by *Bacillus thuringiensis* strain ZS-19, Sci. Rep. 5 (2015) 8784.
[54] H. Liu, W.J. Chen, Z. Xu, S.F. Chen, H. Song, Y. Huang, K. Bhatt, S. Mishra, M. A. Ghorab, L.H. Zhang, et al., Unraveling the degradation mechanism of multiple pyrethroid insecticides by *Pseudomonas aeruginosa* and its environmental bioremediation potential, Environ. Int. 195 (2025) 109221.
[55] S.I. Mulla, F. Ameen, P.N. Tallur, R.N. Bharagava, M. Bangeppagari, S. Eqani, Z. K. Bagewadi, G.D. Mahadevan, C.P. Yu, H.Z. Ninnekar, Aerobic degradation of fenvalerate by a Gram-positive bacterium, *Bacillus flexus* strain XJU-4, 3, Biotech 7 (2017) 320.
[56] Y. Suzuki, M. Yoshida, T. Sugano, A. Shibata, R. Kodaka, T. Fujisawa, T. Katagi, Behavior of cyphenothrin in aquatic environment, J. Pestic. Sci. 42 (2017) 17–24.
[57] Y. Liu, S. Tang, X. Wang, X. Wang, X. Tang, Q. Wu, Z. Huang, J. Ding, A novel thermostable and salt-tolerant carboxylesterase involved in the initial aerobic degradation pathway for pyrethroids in *Glycomyces salinus*, J. Hazard. Mater. 451 (2023) 131128.
[58] W. Zong, W. Su, Q. Xie, Q. Gu, X. Deng, Y. Ren, H. Li, Expression, characterization, and immobilization of a novel SGNH esterase Est882 and its potential for pyrethroid degradation, Front. Microbiol. 13 (2022) 1069754.
[59] A.X. Tang, H. Liu, Y.Y. Liu, Q.Y. Li, Y.M. Qing, Purification and characterization of a novel β-cypermethrin-degrading aminopeptidase from *Pseudomonas aeruginosa* GF31, J. Agric. Food Chem. 65 (2017) 9412–9418.
[60] Y. Zhai, K. Li, J. Song, Y. Shi, Y. Yan, Molecular cloning, purification and biochemical characterization of a novel pyrethroid-hydrolyzing carboxylesterase gene from *Ochrobactrum anthropi* YZ-1, J. Hazard. Mater. 221–222 (2012) 206–212.
[61] C. Diegelmann, J. Weber, R. Heinzel-Wieland, M. Kemme, Characterization of a cypermethrin-degrading *Methylobacterium* sp. strain A-1 and molecular cloning of its carboxylesterase gene, J. Basic. Microb. 55 (2015) 1245–1254.
[62] D. Xu, Y. Gao, B. Sun, T. Ran, L. Zeng, J. He, J. He, W. Wang, Pyrethroid carboxylesterase PytH from *Sphingobium faniae* JZ-2: structure and catalytic mechanism, Appl. Environ. Microbiol. 86 (2020) e02971–e03019.